Study of flavor dependence of the baryon-to-meson ratio in proton-proton collisions at √s=13 TeV

(ALICE Collaboration) Acharya, S.; ...; Erhardt, F.; ...; Gotovac, S; ...; Karatović, D.; ...; Lončar, P.; ...; ...

Journal article, Published version
Rad u časopisu, Objavljena verzija rada (izdavačev PDF)

Permanent link / Trajna poveznica: https://urn.nsk.hr/urn:nbn:hr:217:273154

Download date / Datum preuzimanja: **2024-08-16**

Repository / Repozitorij:

Repository of the Faculty of Science - University of Zagreb

Study of flavor dependence of the baryon-to-meson ratio in proton-proton collisions at $\sqrt{s} = 13$ TeV

S. Acharya *et al.*[*]

(ALICE Collaboration)

The production cross sections of D^0 and Λ_c^+ hadrons originating from beauty-hadron decays (i.e., nonprompt) were measured for the first time at midrapidity ($|y| < 0.5$) by the ALICE Collaboration in proton-proton collisions at a center-of-mass energy $\sqrt{s} = 13$ TeV. They are described within uncertainties by perturbative QCD calculations employing the fragmentation fractions of beauty quarks to baryons measured at forward rapidity by the LHCb Collaboration. The $b\bar{b}$ production cross section per unit of rapidity at midrapidity, estimated from these measurements, is $d\sigma_{b\bar{b}}/dy|_{|y|<0.5} = 83.1 \pm 3.5(\text{stat}) \pm 5.4(\text{syst})^{+12.3}_{-3.2}(\text{extrap})$ μb. The baryon-to-meson ratios are computed to investigate the hadronization mechanism of beauty quarks. The nonprompt Λ_c^+/D^0 production ratio has a similar trend to the one measured for the promptly produced charmed particles and to the p/π^+ and Λ/K_S^0 ratios, suggesting a similar baryon-formation mechanism among light, strange, charm, and beauty hadrons. The p_T-integrated nonprompt Λ_c^+/D^0 ratio is found to be significantly higher than the one measured in e^+e^- collisions.

I. INTRODUCTION

Measurements of open charm- and beauty-meson production in proton-proton (pp) collisions are successfully described by quantum chromodynamics (QCD) calculations based on the factorization of soft (nonperturbative) and hard (perturbative) processes [1–12]. Within the collinear factorization approach, the production cross sections of heavy-flavor hadrons are computed as the convolution of (i) the parton distribution functions (PDFs) of the incoming protons, (ii) the perturbative partonic cross section, and (iii) the fragmentation functions (FFs) describing the transition from the heavy quark to the hadron. The partonic cross section in these calculations is typically computed at next-to-leading order accuracy with all-order resummation of next-to-leading logarithms (e.g., FONLL [13–15] and GM-VFNS [16–21]), but recently calculations at next-to-next-to-leading order (NNLO) also became available [22]. The FFs are instead parametrized from measurements performed in e^+e^- or ep collisions [23], assuming that the hadronization process of charm and beauty quarks is independent of the collision system.

Recent measurements of charm baryon-to-meson production ratios and fragmentation fractions (i.e., the probability of charm quark to fragment into a specific hadron) at midrapidity in pp collisions at LHC energies showed significant deviations from the values measured at e^+e^- and ep colliders [24–32], demonstrating that the assumption of universality of the hadronization process across the collision systems has to be reconsidered. As reported in Ref. [30], the observed baryon-to-meson enhancement also leads to an increase of the derived $c\bar{c}$ production cross section at midrapidity compared to previous measurements, where prompt D-meson cross sections and fragmentation fractions from e^+e^- were used. Models based on the hadronization via coalescence, i.e., recombination of heavy and light quarks close in space and with similar velocity, are able to reproduce the magnitude as well as the p_T dependence of the measured Λ_c^+/D^0 ratio [33,34]. An alternative explanation is provided by statistical hadronization models, if an augmented set of yet unobserved charm-baryon states predicted by the relativistic-quark model [35] and lattice QCD [36] is considered. Moreover, string fragmentation models including color-reconnection mechanisms beyond the leading-color (CLR-BLC) approximation introduce new topologies through the contributions of "junctions" that fragment into baryons, thus providing an augmented baryon production [37]. In the beauty sector, the measurements of Λ_b^0-baryon production relative to that of B mesons at forward rapidity by the LHCb Collaboration show a modification of the fragmentation fractions among collision systems similar

to that observed for charm quarks at midrapidity [38,39]. However, the rapidity-dependent baryon-to-meson enhancement with respect to values measured at e^+e^- and ep colliders is still not fully understood and explored. Different enhancement was observed for the charm baryon-to-meson ratio between midrapidity and forward rapidity for $p_T < 8$ GeV/c and for different colliding systems (i.e., pp, p–Pb) [27,40,41]. Beauty measurements at midrapidity are available only at high transverse momentum ($p_T > 7$ GeV/c) [5,42–48], hence a firm conclusion cannot be drawn.

In this article, the first measurements of the p_T-differential and p_T-integrated production cross sections of D^0 mesons and Λ_c^+ baryons at midrapidity ($|y| < 0.5$) originating from beauty-hadron decays (denoted as nonprompt) in pp collisions at a center-of-mass energy of $\sqrt{s} = 13$ TeV are reported. The differential measurements performed in $1 < p_T < 24$ GeV/c and $2 < p_T < 24$ GeV/c for D^0 and Λ_c^+ hadrons, respectively, are extrapolated down to $p_T = 0$ to compute the p_T-integrated production cross sections and compute the $b\bar{b}$ production cross section at midrapidity. Finally, the nonprompt Λ_c^+/D^0 production ratio is compared with the production ratio of prompt Λ_c^+ and D^0, with the p/π^+ and Λ/K_S^0 ratios, as well as with predictions based on the statistical hadronization model TAMU [49] or the PYTHIA8 Monte Carlo (MC) generator [50] to investigate the hadronization mechanisms of beauty quarks into baryons and mesons.

II. EXPERIMENTAL APPARATUS AND DATA SAMPLE

The description of the ALICE apparatus and of its performance is presented in detail in Refs. [51,52]. The detectors used for the reconstruction of nonprompt charm-hadron decays are the inner tracking system (ITS), the time projection chamber (TPC), and the time-of-flight detector (TOF). These are located in the central barrel, which covers the pseudorapidity interval $|\eta| < 0.9$ inside a solenoid magnet of field strength $B = 0.5$ T. The ITS and the TPC are used for tracking charged particles and reconstructing particle decay vertices. Particle identification (PID) is performed via the measurement of the specific energy loss dE/dx in the TPC and of the flight time with the TOF detector.

The data used for this analysis were collected during pp collisions at $\sqrt{s} = 13$ TeV, with a minimum bias (MB) trigger. The latter requires coincident signals in the two scintillator arrays covering the intervals $2.8 < \eta < 5.1$ (V0A) and $-3.7 < \eta < -1.7$ (V0C). Offline selections were applied to remove background from beam–gas collisions, as described in Ref. [27]. Only events with a primary vertex reconstructed within ± 10 cm from the nominal interaction point along the beam line were analyzed. Events with multiple primary vertices were rejected

in order to remove collision pileup in the same bunch crossing. The remaining undetected pileup is negligible. The selected events correspond to an integrated luminosity $\mathcal{L}_{int} = 31.9 \pm 0.5$ nb^{-1} [53].

III. DATA ANALYSIS

A. D^0 and Λ_c^+ raw yields

The D^0 meson, Λ_c^+ baryon, and their charge conjugates were reconstructed via the hadronic decay channels $D^0 \to K^-\pi^+$ (branching ratio BR = $3.95 \pm 0.03\%$), $\Lambda_c^+ \to pK_S^0$ (BR = $1.59 \pm 0.08\%$, followed by $K_S^0 \to \pi^+\pi^-$ with a BR of $69.20 \pm 0.05\%$), and $\Lambda_c^+ \to pK^-\pi^+$ (BR = $6.28 \pm 0.32\%$) [54]. The D^0-meson and Λ_c^+-baryon candidates were reconstructed by combining pairs or triplets of tracks reconstructed with the proper charge, while for the $\Lambda_c^+ \to pK_S^0$ channel the V-shaped decay of the K_S^0 meson into two pion-track candidates was combined with a proton-track candidate, using a Kalman-Filter vertexing algorithm [55]. All daughter tracks were required to be reconstructed within $|\eta| < 0.8$ and to have at least 70 reconstructed space points in the TPC. For all decay products, at least one cluster was required in either of the two SPD layers. As a consequence of these track-quality selections, the detector acceptance for the candidates falls steeply to zero for $|y| \approx 0.5$ at $p_T \approx 0$ and at $|y| \approx 0.8$ for $p_T > 5$ GeV/c. Thus, a fiducial-acceptance selection $|y| < y_{fid}(p_T)$ was applied, increasing from 0.5 at $p_T = 0$ to the maximum value of 0.8 at $p_T \geq 5$ GeV/c.

A multi-class classification approach based on Boosted Decision Trees (BDT) algorithms provided by the XGBOOST [56,57] library, was used to simultaneously reduce the combinatorial background, and to separate the prompt and nonprompt components for D^0 mesons and Λ_c^+ baryons. Indeed, the inclusive sample of D^0 and Λ_c^+ is dominated by the prompt hadrons and the nonprompt ones are a small fraction which can be enhanced exploiting the larger displacement due to the beauty-hadron decay topology. Signal samples of prompt and nonprompt candidates for the BDT training were obtained from MC simulations produced with the PYTHIA8.243 [50] event generator with the Monash 2013 tune [58]. The generated particles were propagated through the ALICE apparatus using the GEANT3 transport code [59]. Background samples were extracted from the candidate invariant-mass distributions inside the window of $5\sigma < |\Delta M| < 9\sigma$ in data, where ΔM is the difference between the candidate invariant mass and the D^0 (Λ_c^+) mass, and σ is the invariant-mass resolution. Loose selections on the decay kinematics, the decay topology, and the PID of the decay particles were applied to the candidates before the training. The BDTs were trained in each p_T interval using different variables related to the displaced decay-vertex topology and the PID of the decay tracks, similarly as described in Refs. [2,60]. The BDT outputs are related to the candidate's probability to be either prompt or nonprompt D^0 (Λ_c^+) meson (baryon) or

combinatorial background. Selections on the BDT output probabilities of being background and nonprompt were optimized to obtain a high nonprompt D^0 and Λ_c^+ fractions (i.e., $\geq 60\%$ in each p_T interval) while maintaining a reliable signal extraction. The sample of candidates passing the BDT selection is denoted in the following as nonprompt enhanced sample. Based on the selections on the BDT outputs, samples dominated by nonprompt (prompt) candidates were selected by requiring low BDT probability for a candidate to be combinatorial background and a high BDT probability to be nonprompt (prompt).

The D^0 -meson and Λ_c^+ -baryon raw yields were extracted via binned maximum-likelihood fits to the candidate invariant-mass distributions. The fitting function was composed of a Gaussian term to model the signal and an exponential or polynomial function to model the background. In the case of D^0 mesons, an additional term was added for the contribution of signal candidates with the wrong $K - \pi$ mass assignment (reflections), parametrized from simulated candidates [1]. To improve the stability of the fits, the widths of the signal peaks were fixed to the values extracted from the fits of the invariant-mass distributions in the prompt enhanced sample, given the naturally larger abundance of prompt compared to non-prompt candidates. Examples of invariant-mass fits with different contributions of signal from beauty-hadron decays in the $2 < p_T < 4$ GeV/c interval are shown in Fig. 1 for D^0 (top row), $\Lambda_c^+ \to pK_S^0$ (middle row), and $\Lambda_c^+ \to pK^-\pi^+$ (bottom row). The blue solid curves show the total fit function, the red dashed curves show the combinatorial-background contribution, and the green solid lines represent the reflection contribution only for D^0. The fits to the invariant-mass distributions of nonprompt (prompt) enhanced samples are shown in each right (left) panel, indicating the corresponding selection applied on the BDT output score related to the probability to be a nonprompt (prompt) charm hadron.

B. Yield corrections and nonprompt fraction estimate

The nonprompt D^0 and Λ_c^+ p_T-differential cross sections were obtained in the rapidity interval $|y| < 0.5$ as

$$\frac{d\sigma^{\Lambda_c^+(D^0)}}{dp_T dy} = \frac{1}{BR} \times \frac{1}{2c_{\Delta y}(p_T)\Delta p_T} \times \frac{f_{nonprompt} \times N_{raw}}{(Acc \times \epsilon)_{non-prompt}} \times \frac{1}{\mathcal{L}_{int}},$$

$$(1)$$

where N_{raw} is the raw yield (sum of particles and anti-particles), $c_{\Delta y}(p_T)$ and Δp_T represent the width of the rapidity and transverse momentum intervals respectively, BR is the branching ratio of the considered decay mode, the factor of 2 is introduced to obtain the average of particle and antiparticle yields, $f_{nonprompt}$ is the fraction of nonprompt hadrons in the raw yield, $(Acc \times \epsilon)_{non-prompt}$ is

the product of the geometrical acceptance and the reconstruction and selection efficiency for nonprompt hadrons, which increases with p_T from 5% to 25% depending on the BDT selections and decay channel for Λ_c^+ (5% to 40% for D^0), and $\mathcal{L}_{int}$ is the integrated luminosity. The correction factors (Acc $\times \epsilon$) for the detector acceptance and the signal reconstruction and selection efficiency were determined using the aforementioned MC simulations.

A data-driven procedure based on the construction of data samples with different abundances of prompt and nonprompt candidates was used to estimate the fraction $f_{nonprompt}$ of nonprompt D^0 and nonprompt Λ_c^+ hadrons. A set of raw yields (Y_i) can be obtained by varying the selection on the BDT output, which is related to the candidate's probability to be a nonprompt D^0 meson or a nonprompt Λ_c^+ baryon. These raw yields are sensitive to the corresponding (Acc $\times \epsilon$) of prompt and nonprompt D^0 or Λ_c^+ hadrons as follows

$$(Acc \times \epsilon)_i^{prompt} \times N_{prompt}$$
$$+ (Acc \times \epsilon)_i^{nonprompt} \times N_{nonprompt} - Y_i = \delta_i, \quad (2)$$

where δ_i represents a residual that accounts for the equation not holding exactly due to the uncertainties of Y_i, $(Acc \times \epsilon)_i^{nonprompt}$, and $(Acc \times \epsilon)_i^{prompt}$. In the case of $n \geq 2$ sets, a χ^2 function can be defined based on Eq. (2), which can be minimized to obtain the corrected yields of prompt (N_{prompt}) and nonprompt ($N_{nonprompt}$) Λ_c^+ (D^0) hadrons as explained in Ref. [2]. One of the n sets with a high nonprompt component (larger than 50%) was selected as a working point (default), and the corresponding $f_{non-prompt,default}$ fraction (more details in Ref. [2]) can be calculated as

$$f_{non-prompt,default}$$

$$= \frac{(Acc \times \epsilon)_{default}^{nonprompt} \times N_{nonprompt}}{(Acc \times \epsilon)_{default}^{nonprompt} \times N_{nonprompt} + (Acc \times \epsilon)_{default}^{prompt} \times N_{prompt}}.$$

$$(3)$$

Figure 2 shows an example of raw-yield distribution as a function of the BDT-based selection employed in the minimization procedure for D^0 in $2 < p_T < 4$ GeV/c (top left panel), $\Lambda_c^+ \to pK^-\pi^+$ in $4 < p_T < 6$ GeV/c (top right panel), and $\Lambda_c^+ \to pK_S^0$ in $6 < p_T < 8$ GeV/c (bottom left panel). The black markers are the measured raw yields corresponding to a selection on the BDT output related to the candidate's probability of being a nonprompt D^0 (Λ_c^+) meson (baryon). The leftmost data point of each distribution corresponds to the loosest applied selection, while the rightmost one corresponds to the tightest selection, which preferentially selects nonprompt candidates. The prompt and nonprompt components, obtained for each
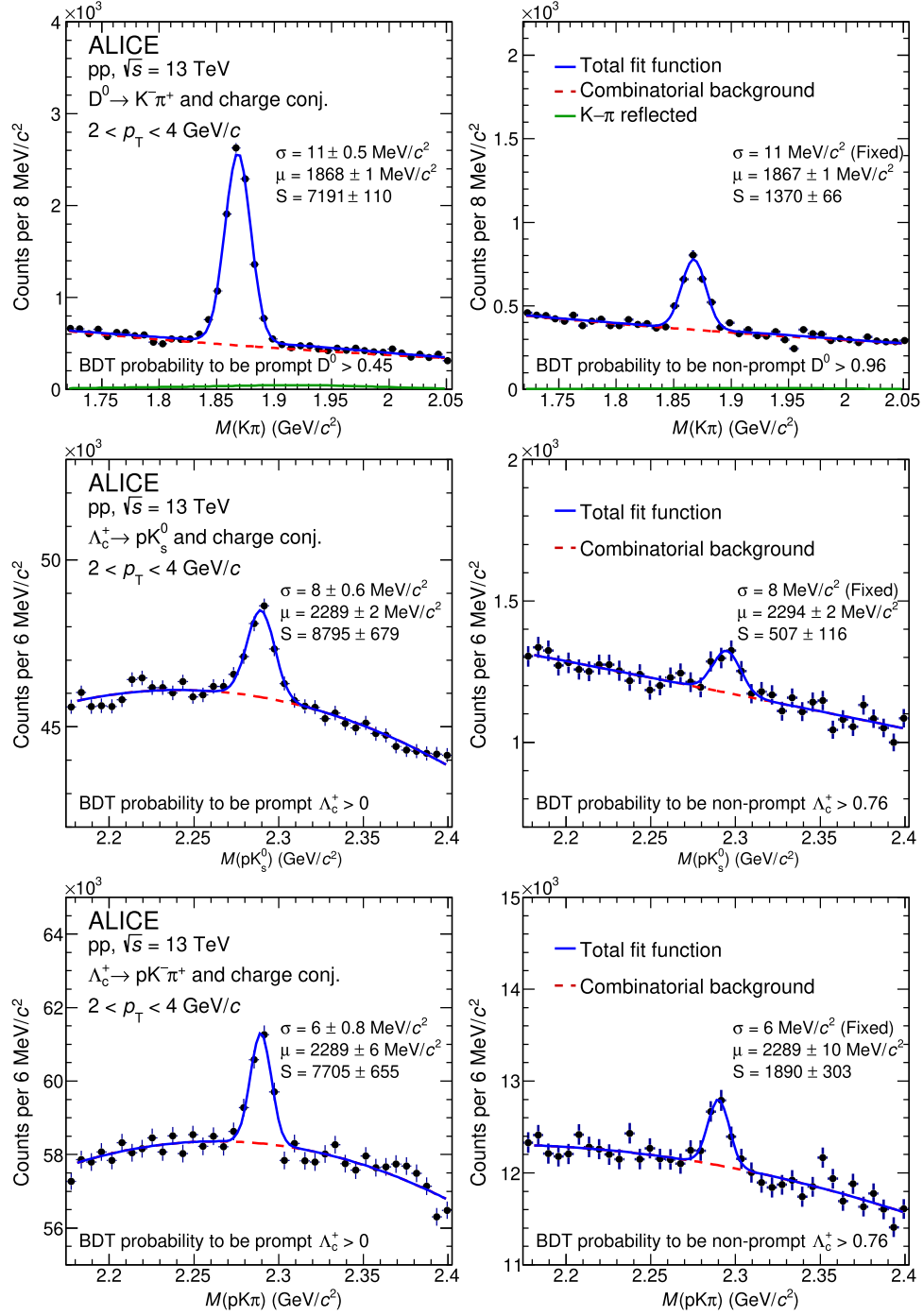
FIG. 1. Invariant-mass distributions of the D^0- and Λ_c^+-hadron candidates and their charge conjugates produced in pp collisions at $\sqrt{s} = 13$ TeV and reconstructed at midrapidity, shown in a selected p_T range. The values for the Gaussian mean μ, width σ, and raw yield S are reported. Top row: $D^0 \to K^-\pi^+$ meson candidates measured in the $2 < p_T < 4$ GeV/c interval. Middle row: $\Lambda_c^+ \to pK_S^0$ baryon candidates measured in the $2 < p_T < 4$ GeV/c interval. Bottom row: $\Lambda_c^+ \to pK^-\pi^+$ baryon candidates measured in the $2 < p_T < 4$ GeV/c interval. The corresponding BDT probability minimum threshold for the candidate selection is reported. The left (right) column corresponds to the prompt (nonprompt) D^0- and Λ_c^+-hadron candidates enriched sample.

BDT-based selection from the minimization procedure as $(\mathrm{Acc} \times \epsilon)_i^{\mathrm{prompt}} \times N_{\mathrm{prompt}}$ and $(\mathrm{Acc} \times \epsilon)_i^{\mathrm{nonprompt}} \times N_{\mathrm{nonprompt}}$, are represented by the red and blue filled histograms, respectively, while their sum is reported by the green histogram. The $f_{\mathrm{nonprompt}}$ fractions obtained for D^0, $\Lambda_c^+ \to pK^-\pi^+$, and $\Lambda_c^+ \to pK_S^0$, computed for the default selections with the formula in Eq. (3) are reported as a function of p_T in the bottom right panel of Fig. 2.
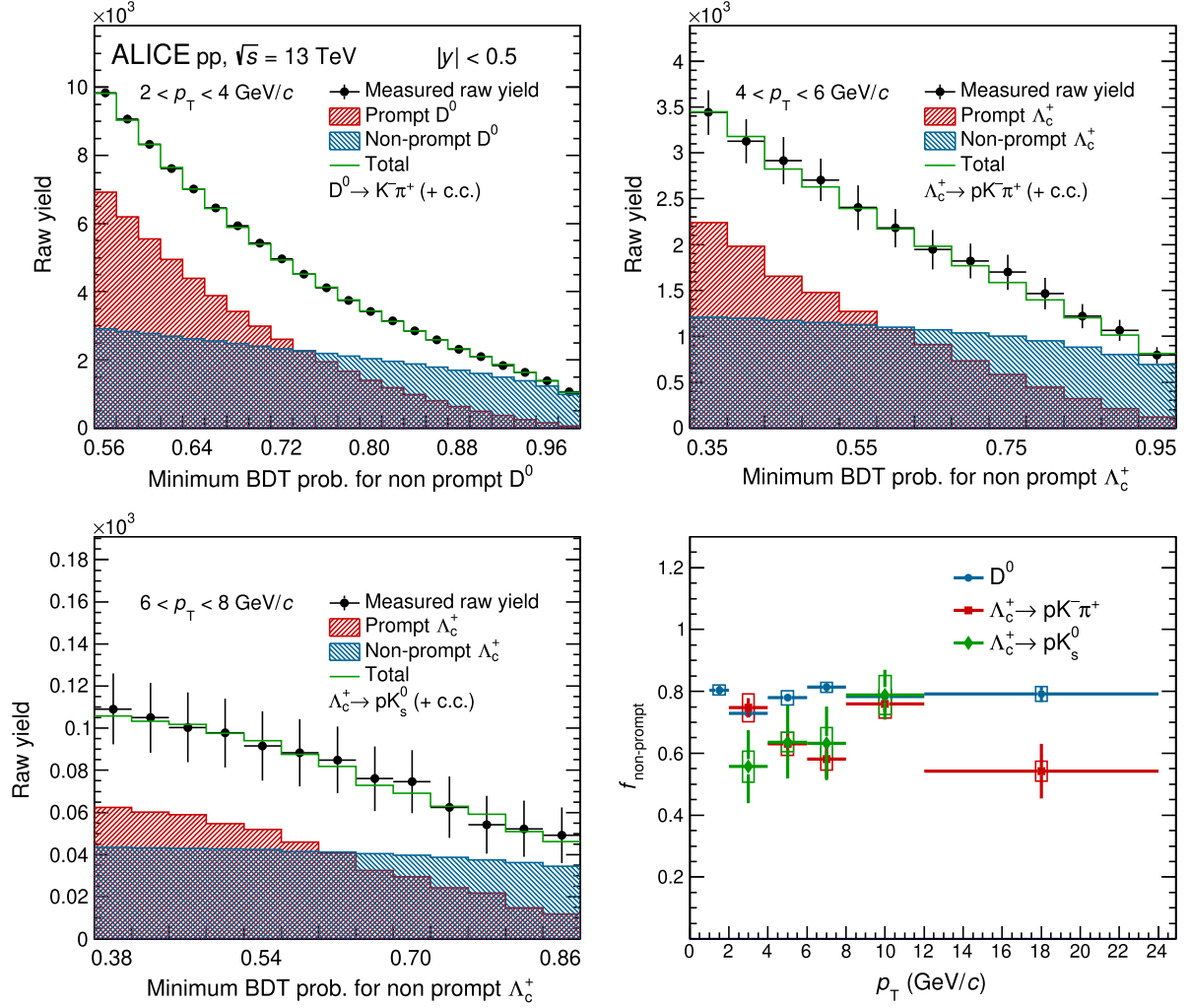
FIG. 2. Raw-yield distribution as a function of the BDT-based selection employed in the χ^2-minimization procedure adopted for the determination of $f_{\text{nonprompt}}$ of D^0 in $2 < p_T < 4$ GeV/c (top left panel), $\Lambda_c^+ \to pK^-\pi^+$ in $4 < p_T < 6$ GeV/c (top right panel), and $\Lambda_c^+ \to pK_S^0$ in $6 < p_T < 8$ GeV/c (bottom left panel). Bottom right panel: $f_{\text{nonprompt}}$ fraction as function as p_T obtained for the set of selection criteria adopted in the analysis of for nonprompt D^0, $\Lambda_c^+ \to pK^-\pi^+$, and $\Lambda_c^+ \to pK_S^0$ hadrons.

IV. SYSTEMATIC UNCERTAINTIES

The systematic uncertainties of the nonprompt Λ_c^+ and D^0 cross sections were studied for the different decay channels, which depend on p_T. The contributions from the raw-yield extraction were evaluated by repeating the invariant-mass fits, varying the fit interval, the functional form of the background fit function, and the width of the Gaussian function used to model the signal peaks. The latter was varied within the uncertainties obtained from the fits of the invariant-mass distributions of the prompt enhanced sample. The relative uncertainty from this contribution varies in the range 1%–3% for D^0 and 4%–11% for Λ_c^+. The uncertainties of the track reconstruction efficiency were estimated by considering the uncertainty due to track quality selections and the uncertainty due to the TPC–ITS track matching efficiency as discussed in Ref. [2]. It ranges from 3.5% to 5% for D^0 and from

4% to 7% for Λ_c^+. The systematic uncertainties of the nonprompt fractions were evaluated by varying the configuration and the number of BDT selections employed in the data-driven method and amounts to 2%–3% for D^0 and 5%–9% for Λ_c^+. The selection efficiency uncertainties, ranging from 2% to 4% for D^0 and 4% to 10% for Λ_c^+, were studied by repeating the analyses using different BDT working points. The systematic uncertainties of the PID selection efficiency were found to be negligible, similar to what observed for prompt charm hadrons [60]. The systematic effects due to a possible difference between the real and simulated charm and beauty hadron p_T spectra, were estimated by evaluating the selection efficiency after reweighting the p_T shape from the PYTHIA8.243 event generator to match the one from FONLL calculations [13–15] for prompt and nonprompt D^0. For the Λ_c^+ the reweighting was defined to match the p_T shape of D^0 and B

mesons from FONLL multiplied by the Λ_c^+/D^0 yield ratio from ALICE [27] and the Λ_b^0/B yield ratio from LHCb [39], respectively. The weights were applied to the p_T distributions for prompt hadrons and to the mother beauty-hadron particles in the case of nonprompt hadrons. The systematic uncertainty from this contribution varies in the range 1%–4% for D^0 and 4%–5% for Λ_c^+. In addition, the imperfect apparatus material budget description in the MC simulation, particularly relevant for the effects of the absorption of protons, might result in a bias in the estimation of the Λ_c^+ efficiencies. It was evaluated by comparing the corrected yields of charged pions, kaons, and protons using a standard MC production and one with the material budget increased artificially by 10%. The assigned systematic uncertainty is 2%. Further p_T-independent uncertainties from the BR [61] and the luminosity [53] were considered. The total uncertainties, 5%–8% for D^0 and 12%–17% for Λ_c^+, were calculated as the quadratic sum of the contributions of the different sources.

V. RESULTS

A. Production cross sections

The p_T-differential production cross sections of non-prompt Λ_c^+ baryons and D^0 mesons are shown in Fig. 3. The nonprompt Λ_c^+ cross section was obtained by computing a

weighted average of the results from the analyses of the $\Lambda_c^+ \to pK_S^0$ and $\Lambda_c^+ \to pK^-\pi^+$ decay channels, using the inverse of the quadratic sum of the relative statistical and uncorrelated systematic uncertainties as weights. The systematic uncertainties related to the tracking, luminosity, and generated p_T spectrum in the MC simulations are treated as correlated between the two decay channels, the uncertainty of the branching ratios as partially correlated as described in Ref. [54], while all the other sources of systematic uncertainties are considered uncorrelated. The data points are compared with theoretical models based on the B-meson cross section predicted by FONLL calculations in the left panel and to the TAMU statistical hadronization model [49] in the right panel. In the FONLL-based predictions, the beauty-quark fragmentation fraction to B mesons, $f(b \to B)$, was taken from e^+e^- collisions [54]. For the Λ_b^0 baryon, $f(b \to B)_{e^+e^-} \times (f(b \to \Lambda_b^0)/f(b \to B))_{LHCb}$ was used, where the p_T-differential ratio Λ_b^0/B was measured by the LHCb Collaboration in pp collisions [39]. It has to be noted that the usage of the p_T-differential fragmentation fractions ratio $(f(b \to \Lambda_b^0)/f(b \to B))_{LHCb}$ combined with the $f(b \to B)$ from e^+e^- collisions enlarges the total beauty production cross section compared to the one predicted by FONLL calculations. In the TAMU model instead, the branching fractions of beauty quarks to the different hadron species are assumed to follow the relative thermal densities calculated
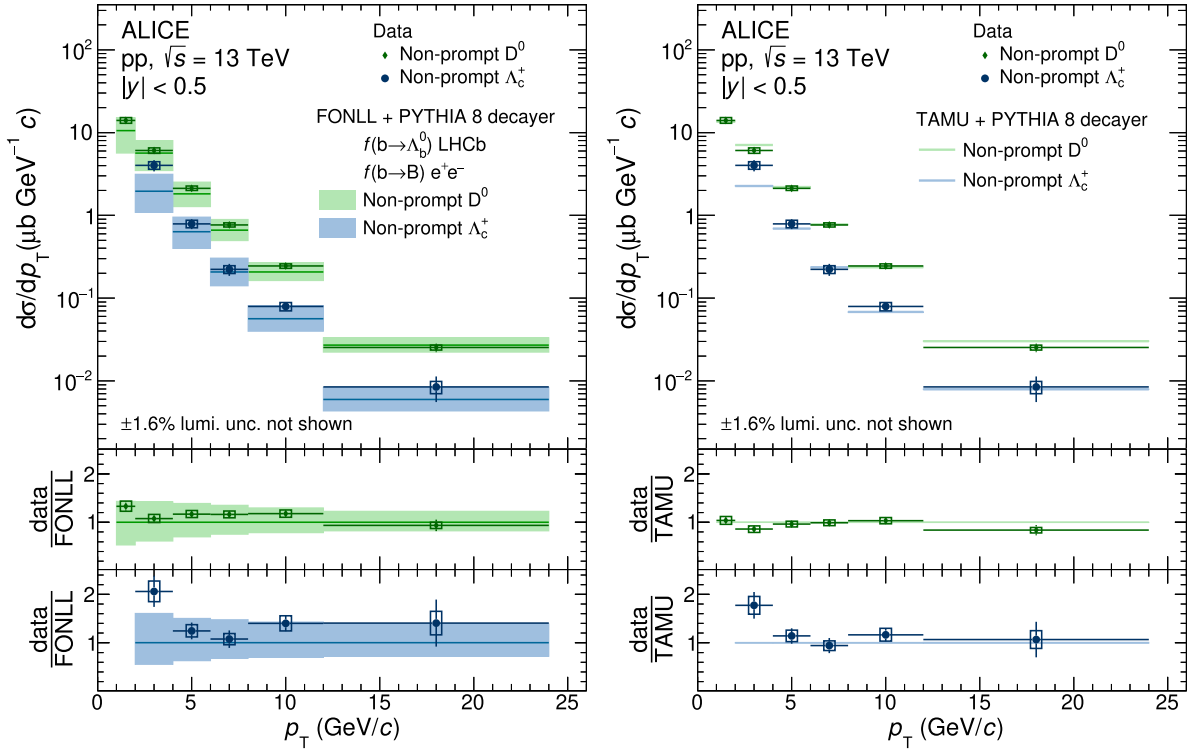

FIG. 3. p_T-differential production cross sections of nonprompt D^0 and Λ_c^+ hadrons in pp collisions at $\sqrt{s} = 13$ TeV compared with predictions obtained with FONLL calculations [13–15] adopting $f(b \to B)$ and $f(b \to \Lambda_b^0)$ fragmentation fractions measured in e^+e^- collisions [61] and LHCb Collaboration [39] (left panel) and the TAMU model [49] (right panel) combined with PYTHIA8 [50,58] for the $h_b \to h_c + X$ decay kinematics.

with the statistical hadronization model and an enriched set of heavy-flavor hadron states is obtained from the relativistic-quark model [35]. The p_T distribution is obtained from the one of beauty quarks, convoluted to the fragmentation functions as implemented in FONLL calculations. In this case, the $b\bar{b}$ production cross section at midrapidity is a parameter of the model, fixed to $d\sigma_{b\bar{b}}/dy|_{y=0} = 85.3$ μb.

The resulting beauty-hadron cross sections of both models were then folded with the $h_b \to h_c + X$ decay kinematics (where h_c and h_b denote a generic hadron species containing either a charm or beauty quark) and branching ratios provided by the PYTHIA8 decayer, in order to obtain the nonprompt D^0 and Λ_c^+ cross sections. In the left panel, the uncertainties in the model are those of the FONLL calculation, which arise from the choice of the normalization and factorization scales, and the mass of the beauty quark, combined with the uncertainties of the CTEQ6.6 PDFs. The nonprompt D^0 cross section is in agreement with FONLL + PYTHIA8 and TAMU + PYTHIA8 predictions over the whole p_T range, while the nonprompt Λ_c^+ cross section shows a hint of underestimation at low p_T ($2 < p_T < 4$ GeV/c) by both models.

The measured visible cross sections of nonprompt Λ_c^+ and D^0 hadrons were computed by integrating the measured p_T-differential cross sections in the measured p_T range. All the systematic uncertainties were propagated as fully correlated among the measured p_T intervals, except for the raw-yield extraction uncertainty. As the p_T-differential cross sections predicted by FONLL + PYTHIA8 were found to be compatible with the measurements, they were assumed to provide an accurate description of the p_T shape also outside of the measured p_T range. Therefore, the visible cross section was then extrapolated to the full p_T range, using an extrapolation factor computed as the ratio of the p_T-integrated cross sections predicted by FONLL + PYTHIA8 integrated over $p_T > 0$ and that in the measured p_T interval. The systematic uncertainty of the extrapolation factors was computed considering (i) the FONLL uncertainties, (ii) the $f(b \to h_b)$ fragmentation fractions uncertainties, and (iii) the branching ratios uncertainties of the $h_b \to h_c + X$ decays. The second source was estimated by using different sets of beauty fragmentation fractions (from e^+e^-, $p\bar{p}$ collisions [54], or those measured by LHCb [39]), while for the third one the branching ratios implemented in PYTHIA8 were reweighted in order to reproduce the measured values reported in Ref. [54]. The resulting

extrapolation factors are $\alpha_{\text{extrap}}^{D^0} = 1.241_{-0.047}^{+0.009}$ and $\alpha_{\text{extrap}}^{\Lambda_c^+} = 1.847_{-0.152}^{+0.108}$ for D^0 mesons and Λ_c^+ baryons, respectively. The p_T-integrated cross sections are reported in Table I and compared to FONLL + PYTHIA8 calculations, which describe the measurements within the uncertainties.

Similarly, the $b\bar{b}$ production cross section per unit of rapidity at midrapidity was obtained summing the visible cross sections previously computed and then using an extrapolation factor to account for the unmeasured p_T regions and hadrons. This factor was computed as the ratio of the beauty cross section and the visible cross section of a nonprompt charm hadron, estimated with FONLL + PYTHIA8 as follows

$$\alpha_{\text{extrap}}^{b\bar{b}} = \frac{d\sigma_{b\bar{b}}^{\text{FONLL}}/dy|_{|y|<0.5}}{d\sigma_{h_c \leftarrow b}^{\text{FONLL+PYTHIA8}}/dy|_{|y|<0.5}(p_T^{\min h_c} < p_T < p_T^{\max h_c})}.$$

(4)

The extrapolation factor for the D^0 meson was found to be $\alpha_{\text{extrap}}^{b\bar{b},D^0} = 2.106_{-0.014}^{+0.366}$, while the one for Λ_c^+ baryons $\alpha_{\text{extrap}}^{b\bar{b},\Lambda_c^+} = 10.98_{-1.34}^{+0.87}$. The systematic uncertainty of the extrapolation factor includes the same sources considered for the extrapolation of the single-hadron production cross sections. In addition, a correction due to the difference between the rapidity distributions of beauty quarks and beauty hadrons, and between the $b\bar{b}$ pairs and beauty quarks was applied. The first factor was evaluated to be unity in the relevant rapidity range based on FONLL calculations with 1% uncertainties evaluated from the difference between FONLL and PYTHIA8. The second correction factor is the ratio $(d\sigma_{b\bar{b}}/dy)/(d\sigma_b/dy) = 1.06 \pm 0.01$ in $|y| < 0.5$, which was estimated from POWHEG simulations [62]. The uncertainty was assigned by varying the factorization and renormalization scales in the POWHEG calculation and using the CT10NLO [63] and CT14NLO [64] PDFs, alternatively to the default one (CTEQ6.6). The $d\sigma_{b\bar{b}}/dy$ was computed separately from the measurements of nonprompt D^0 and Λ_c^+ hadrons were then averaged using the inverse of the quadratic sum of the absolute statistical and uncorrelated systematic uncertainties as weights. The systematic uncertainties related to the tracking uncertainty and the extrapolation uncertainties related to FONLL and the beauty fragmentation fractions were treated as fully correlated among the two hadron species, while all the

TABLE I. Production cross sections at midrapidity per unit of rapidity $(d\sigma/dy)_{|y|<0.5}$ in pp collisions at $\sqrt{s} = 13$ TeV of nonprompt Λ_c^+ and D^0 hadrons and $b\bar{b}$ pairs $(d\sigma_{b\bar{b}}/dy)_{|y|<0.5}$ compared to pQCD calculations [13–15,22].

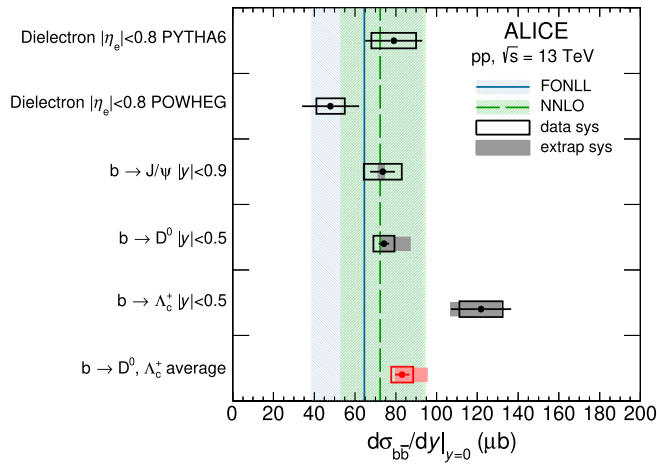|	Measurement (μb)	FONLL (μb) [13–15]	NNLO (μb) [22]
D^0	$41.3 \pm 1.5(\text{stat}) \pm 2.9(\text{syst})_{-1.6}^{+0.3}(\text{extrap})$	34 ± 14	$\cdots$
Λ_c^+	$19.1 \pm 2.3(\text{stat}) \pm 1.7(\text{syst})_{-1.5}^{+1.0}(\text{extrap})$	11_{-5}^{+7}	$\cdots$
$b\bar{b}$	$83.1 \pm 3.5(\text{stat}) \pm 5.4(\text{syst})_{-3.2}^{+12.3}(\text{extrap})$	65_{-26}^{+28}	72_{-20}^{+22}

FIG. 4. Beauty production cross section per rapidity unit at midrapidity obtained from from dielectron [66] and nonprompt J/ψ [3], D^0, and Λ_c^+ hadrons measured in pp collisions at $\sqrt{s} = 13$ TeV compared to FONLL [13–15] and NNLO [22] predictions. The average $d\sigma_{b\bar{b}}/dy$ of the estimates from the D^0 and Λ_c^+ hadrons is also reported.

other sources as uncorrelated. The resulting $b\bar{b}$ production cross section per unit of rapidity at midrapidity is compatible with the predictions from FONLL and NNLO calculations, as reported in Table I. The NNLO predictions are however closer to the measurement and have smaller uncertainties than the FONLL ones, as expected by the higher perturbative accuracy. The measurement is also compatible with previous estimates based on the measurements of dielectrons [65,66] and nonprompt J/ψ mesons [3].

Figure 4 shows the $b\bar{b}$ production cross section per unit rapidity at midrapidity estimated from the production cross sections of nonprompt D^0 and Λ_c^+ hadrons in pp collisions at $\sqrt{s} = 13$ TeV compared to the previous values based on dielectron and nonprompt J/ψ -meson measurements. The experimental results are also compared with the predictions provided by FONLL and NNLO perturbative QCD calculations.

B. Baryon-to-meson ratios

The ratio of the p_T -differential production cross sections of nonprompt Λ_c^+ and D^0 hadrons is shown in Fig. 5. In the left panel, the data are compared with theoretical predictions obtained with FONLL calculations [13–15] and PYTHIA8 [50,58] for the description of the decay kinematics and branching ratios. They are obtained using fragmentation fractions from e^+e^- collisions [61] for the B mesons and the $f(b \rightarrow \Lambda_b^0)/f(b \rightarrow B)$ fragmentation fraction ratio measured by the LHCb Collaboration [39]. The contributions of nonprompt Λ_c^+ baryons originating from B mesons and Λ_b^0 baryons are reported separately to show that the largest contribution is represented by the beauty baryons, while the B mesons contribute only marginally to the nonprompt Λ_c^+ production cross section. Hence, it is possible to inquire the hadronization of beauty quarks into Λ_b^0 baryons through the nonprompt Λ_c^+. In the right panel of the same figure the data are compared with the p_T-differential ratio between prompt Λ_c^+ and D^0 hadrons. The two measurements are compatible in their common p_T range, with a tension of less than two standard deviations in $2 < p_T < 4$ GeV/c, where the ratio of nonprompt hadrons
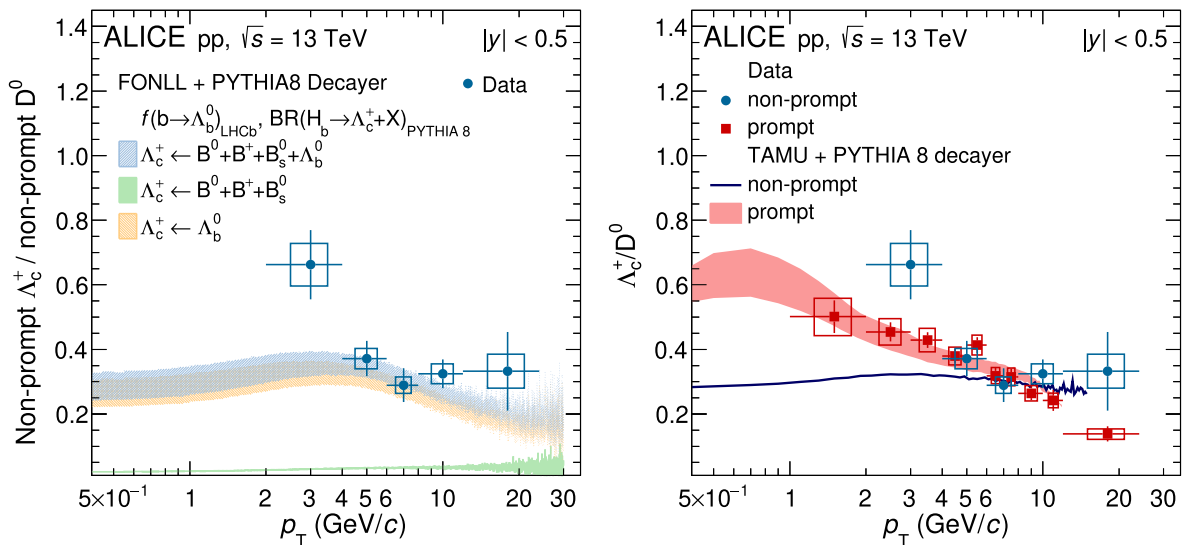
FIG. 5. Left: p_T-differential ratios of nonprompt Λ_c^+- and D^0-hadron cross sections compared with predictions obtained with FONLL calculations [13–15] and PYTHIA8 [50,58] for the $h_b \rightarrow h_c + X$ decay kinematics. The contributions from beauty mesons and from the Λ_b^0 baryon are depicted separately. Right: p_T-differential ratios of prompt [27] and nonprompt Λ_c^+- and D^0-hadron cross sections compared with predictions obtained with the TAMU model [36,49] and PYTHIA8 for the $h_b \rightarrow h_c + X$ decay kinematics.

is higher than the one of promptly produced hadrons. The experimental data are also compared to the predictions obtained with the TAMU model combined with PYTHIA8 to describe the $h_b \rightarrow h_c + X$ decay kinematics, in the case of nonprompt production. The prediction for prompt charm hadrons has an error band representing the uncertainty on the BR of excited charm baryons decaying into Λ_c^+, not included in the one for nonprompt hadrons. The measured nonprompt Λ_c^+/D^0 ratio is rather well described for $p_T > 4$ GeV/c given the current uncertainties, while it is underestimated for $2 < p_T < 4$ GeV/c. The prompt charm and beauty ratios are described by the TAMU calculations within the uncertainties for the whole measured p_T interval.

Figure 6 shows the p_T -differential nonprompt Λ_c^+/D^0 yield ratio at midrapidity ($|y| < 0.5$) in pp collisions at $\sqrt{s} = 13$ TeV compared with the measurements of prompt Λ_c^+/D^0 [27], Λ/K_S^0 [67], and p/π^+ [67] ratios at the same energy and rapidity interval, and with the $\Lambda_b^0/(B^0 + B^+)$ yield ratio measured by LHCb at forward rapidity

($2.5 < y < 4$). The $\Lambda_b^0/(B^0 + B^+)$ ratio is a bit lower than the one between nonprompt Λ_c^+ and D^0 mesons, however it has to be considered that the normalization is slightly different. In the LHCb result the production cross sections of B^0 and B^+ mesons, i.e., the total yield of nonstrange B mesons is used, while the nonprompt D^0, used in this ratio, accounts for about 70% of the nonstrange D mesons. Also the fraction of B^0 and B^+ mesons decaying to Λ_c^+ and D_s^+, as well as the Λ_b^0 and B_s^0 hadrons decaying to D^0 mesons influence the ratio. In addition, in the nonprompt Λ_c^+/D^0 ratio, the $h_b \rightarrow h_c + X$ decay kinematics is expected to slightly modify the p_T dependence compared to the one of the ratio between beauty hadrons. Interestingly, all the measurements for beauty, charm, and strange hadrons show a similar trend as a function of p_T and are compatible within the uncertainties. The p/π^+ production ratio also features a similar p_T dependence, however it is lower in absolute terms. The experimental values are compared with the corresponding predictions obtained with PYTHIA8 simulations, using different tunes and the same rapidity ranges
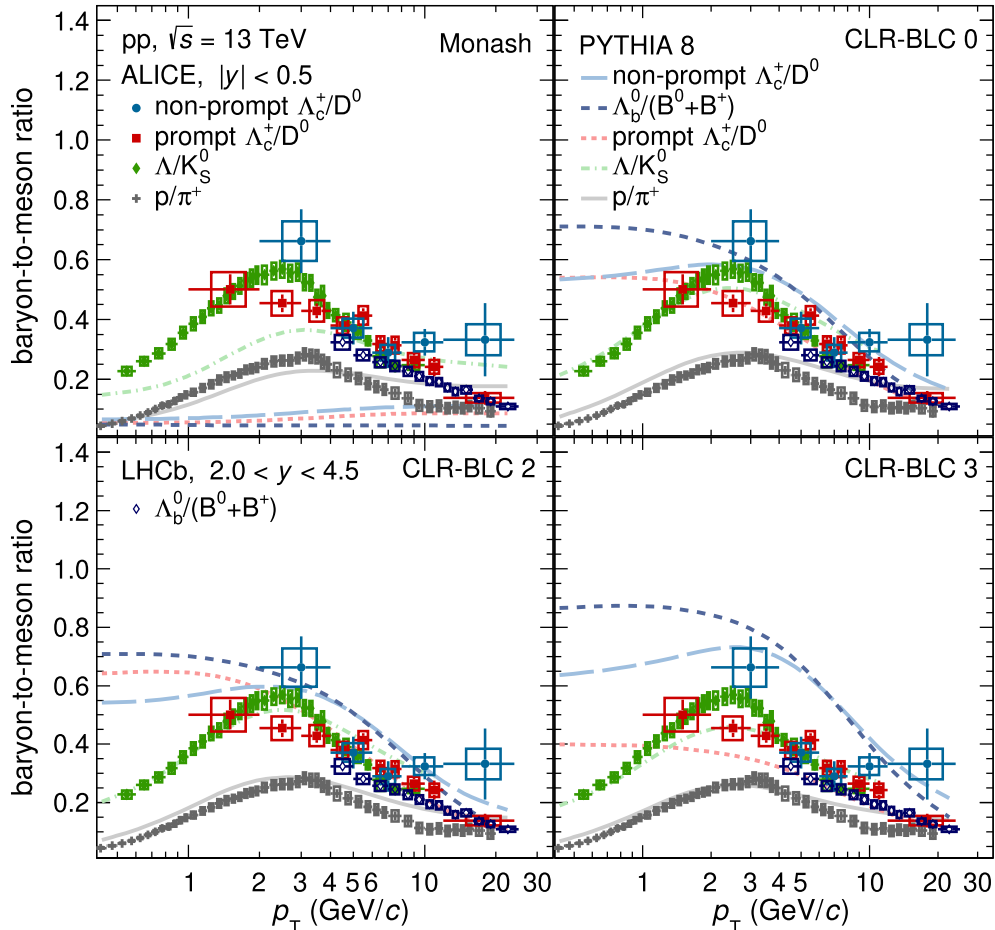
FIG. 6.   Non-prompt Λ_c^+/D^0, prompt Λ_c^+/D^0 [27], Λ/K_S^0 [67], and p/π^+ [67] ratios measured in pp collisions at $\sqrt{s} = 13$ TeV at midrapidity ($|y| < 0.5$) compared with the $\Lambda_b^0/(B^0 + B^+)$ ratio measured by the LHCb Collaboration at forward rapidity ($2.5 < y < 4$) [39] and with predictions obtained with the PYTHIA8 MC generator with the Monash 2013 tune [50,58] and the CLR-BLC modes 0, 2, and 3 [37] in the corresponding rapidity range with respect to data.

TABLE II. p_T-integrated Λ_c^+/D^0 production ratio measured at midrapidity ($|y| < 0.5$) in pp collisions at $\sqrt{s} = 13$ TeV and in e^+e^- collisions at LEP [68] for prompt and nonprompt production.

	ALICE	LEP average [68]
Prompt Λ_c^+/D^0	$0.49 \pm 0.02(\text{stat})^{+0.05}_{-0.04}(\text{syst})^{+0.01}_{-0.03}(\text{syst})$ [60]	0.105 ± 0.013
Nonprompt Λ_c^+/D^0	$0.47 \pm 0.06(\text{stat}) \pm 0.04(\text{syst})^{+0.03}_{-0.04}(\text{extrap})$	0.124 ± 0.016

of the experimental results. In the top-left panel, the results obtained with the Monash 2013 tune [58], which implements a fragmentation process tuned to reproduce the measurements in e^+e^- collisions, is reported. Here, all the baryon-to-meson ratios are underestimated by PYTHIA8 except for the p/π^+ ratio for which the model prediction is rather good at low p_T. A better agreement is instead obtained with the CLR-BLC tunes (i.e., Mode 0, 2, and 3), shown in the other three panels of Fig. 6. These three tunes are characterized by different constraints on the time dilation and causality, as defined in Ref. [37]. The time parameters are relevant in this model, because two strings can reconnect if they are able to resolve each other during the time between their formation and hadronization, taking also into account time-dilation effects caused by relative boosts. The Mode 0 and 2 settings, reported in the top-right and bottom-left panels of Fig. 6 respectively, predict a similar baryon-to-meson ratio for the strange, charm, and beauty flavors for $p_T > 2$ GeV/c and a significantly higher ratio for heavy-flavor hadrons than strange hadrons for lower p_T (e.g., a factor three is predicted at $p_T \approx 400$ MeV/c). Despite the agreement with the data is significantly improved compared to the Monash tune, the measurements of beauty hadrons are overestimated for $p_T \lesssim 10$ GeV/c. Instead, the Mode 3 (bottom-right panel of Fig. 6) underestimates the ratio for charm hadrons for $p_T \lesssim 12$ GeV/c and overestimates that of beauty hadrons in the same p_T interval, quantitatively more than the other two CLR-BLC modes. The features, observed in all comparisons with PYTHIA8 tunes, indicate that more precise measurements of the baryon-to-meson ratios, especially those including beauty-hadron measurements at very low p_T ($p_T < 2$ GeV/c) are crucial for tuning the model parameters involving the reconnection of quarks via junction topologies and to possibly validate this as the mechanism responsible of the baryon enhancement observed in hadron collisions compared to e^+e^- collisions. It is worth pointing out that other theoretical models are proposed to describe the enhancement, based on different hadronization mechanisms (e.g., recombination).

The p_T-integrated nonprompt Λ_c^+/D^0 ratio was computed by dividing the p_T-integrated cross sections reported in Table I. All the systematic uncertainties, except for those related to the tracking efficiency, were propagated as uncorrelated in the ratio. The resulting value is compatible with the one measured for promptly produced particles and significantly higher than that

measured in e^+e^- collisions at LEP [68]. All the values are reported in Table II.

VI. CONCLUSIONS

In summary, the p_T-differential and p_T-integrated production cross sections of nonprompt Λ_c^+ and D^0 hadrons were measured for the first time at midrapidity in pp collisions at $\sqrt{s} = 13$ TeV. The results are compatible with the theoretical models based on FONLL calculations with the $f(b \to \Lambda_b^0)$ and $f(b \to B)$ fragmentation fractions measured by LHCb and at e^+e^-, respectively, suggesting a similar beauty-baryon enhancement at forward and midrapidity in pp collisions. Furthermore, the results are in agreement with the TAMU statistical hadronization model for the relative abundances of different beauty hadron species. The extrapolated $b\bar{b}$ production cross section at midrapidity per unit of rapidity is found to be compatible with pQCD calculations with FONLL and NNLO accuracy. The measured baryon-to-meson ratios of light flavor, strange, charm, and beauty hadrons show a similar p_T trend. In addition, all ratios, except the p/π^+, are significantly higher than the values measured in e^+e^- collisions. The p_T-differential baryon-to-meson ratios have been compared to predictions of the TAMU statistical hadronization model and to the PYTHIA8 simulations, that include the color-reconnection mechanism in the string fragmentation and indicate that all the flavors have to be considered simultaneously in order to obtain the best tuning of the model parameters involving the reconnection of quarks via junction topologies. This feature asks for more precise results, including a direct measurement of beauty hadrons especially in the same p_T and rapidity range and the $p_T < 4$ GeV/c region, which can be reached with the data collected in the LHC Run 3 data taking period.

ACKNOWLEDGMENTS

---

[1] S. Acharya *et al.* (ALICE Collaboration), Measurement of D^0, D^+, D^{*+} and D_s^+ production in pp collisions at $\sqrt{s} = 5.02$ TeV with ALICE, Eur. Phys. J. C **79**, 388 (2019).

[2] S. Acharya *et al.* (ALICE Collaboration), Measurement of beauty and charm production in pp collisions at $\sqrt{s} = 5.02$ TeV via nonprompt and prompt D mesons, J. High Energy Phys. 05 (2021) 220.

[3] S. Acharya *et al.* (ALICE Collaboration), Prompt and nonprompt J/ψ production cross sections at midrapidity in proton-proton collisions at $\sqrt{s} = 5.02$ and 13 TeV, J. High Energy Phys. 03 (2022) 190.

[4] S. Acharya *et al.* (ALICE Collaboration), Measurement of electrons from semileptonic heavy-flavour hadron decays at midrapidity in pp and Pb–Pb collisions at $\sqrt{s_{NN}} = 5.02$ TeV, Phys. Lett. B **804**, 135377 (2020).

[5] V. Khachatryan *et al.* (CMS Collaboration), Measurement of the total and differential inclusive B^+ hadron cross sections in pp collisions at $\sqrt{s} = 13$ TeV, Phys. Lett. B **771**, 435 (2017).

[6] A. M. Sirunyan *et al.* (CMS Collaboration), Nuclear modification factor of D^0 mesons in PbPb collisions at $\sqrt{s_{NN}} = 5.02$ TeV, Phys. Lett. B **782**, 474 (2018).

[7] A. M. Sirunyan *et al.* (CMS Collaboration), Studies of beauty suppression via nonprompt D^0 mesons in Pb-Pb collisions at $Q^2 = 4$ GeV^2, Phys. Rev. Lett. **123**, 022001 (2019).

[8] R. Aaij *et al.* (LHCb Collaboration), Measurements of prompt charm production cross-sections in pp collisions at $\sqrt{s} = 13$ TeV, J. High Energy Phys. 03 (2016) 159; 09 (2016) 13; 05 (2017) 74.

[9] R. Aaij *et al.* (LHCb Collaboration), Measurements of prompt charm production cross-sections in pp collisions at $\sqrt{s} = 5$ TeV, J. High Energy Phys. 06 (2017) 147.

[10] R. Aaij *et al.* (LHCb Collaboration), Measurement of the $B^\pm$ production cross-section in pp collisions at $\sqrt{s} = 7$ and 13 TeV, J. High Energy Phys. 12 (2017) 026.

[11] G. Aad *et al.* (ATLAS Collaboration), Measurement of $D^{*\pm}$, $D^\pm$ and $D_s^\pm$ meson production cross sections in pp collisions at $\sqrt{s} = 7$ TeV with the ATLAS detector, Nucl. Phys. **B907**, 717 (2016).

[12] ALICE Collaboration, The ALICE experiment—A journey through QCD, arXiv:2211.04384.

[13] M. Cacciari, M. Greco, and P. Nason, The p_T spectrum in heavy flavor hadroproduction, J. High Energy Phys. 05 (1998) 007.

[14] M. Cacciari, S. Frixione, and P. Nason, The p_T spectrum in heavy flavor photoproduction, J. High Energy Phys. 03 (2001) 006.

[15] M. Cacciari, S. Frixione, N. Houdeau, M. L. Mangano, P. Nason, and G. Ridolfi, Theoretical predictions for charm and bottom production at the LHC, J. High Energy Phys. 10 (2012) 137.

[16] B. Kniehl, G. Kramer, I. Schienbein, and H. Spiesberger, Inclusive $D^{*\pm}$ production in $p\bar{p}$ collisions with massive charm quarks, Phys. Rev. D **71**, 014018 (2005).

[17] B. Kniehl, G. Kramer, I. Schienbein, and H. Spiesberger, Inclusive charmed-meson production at the CERN LHC, Eur. Phys. J. C **72**, 2082 (2012).

[18] M. Benzke, M. Garzelli, B. Kniehl, G. Kramer, S. Moch, and G. Sigl, Prompt neutrinos from atmospheric charm in the general-mass variable-flavor-number scheme, J. High Energy Phys. 12 (2017) 021.

[19] G. Kramer and H. Spiesberger, Study of heavy meson production in p–Pb collisions at $\sqrt{s} = 5.02$ TeV in the general-mass variable-flavour-number scheme, Nucl. Phys. **B925**, 415 (2017).

[20] I. Helenius and H. Paukkunen, Revisiting the D-meson hadroproduction in general-mass variable flavour number scheme, J. High Energy Phys. 05 (2018) 196.

[21] P. Bolzoni and G. Kramer, Inclusive charmed-meson production from bottom hadron decays at the LHC, J. Phys. G **41**, 075006 (2014).

[22] S. Catani, S. Devoto, M. Grazzini, S. Kallweit, and J. Mazzitelli, Bottom-quark production at hadron colliders: Fully differential predictions in NNLO QCD, J. High Energy Phys. 03 (2021) 029.

[23] E. Braaten, K.-m. Cheung, S. Fleming, and T. C. Yuan, Perturbative QCD fragmentation functions as a model for heavy quark fragmentation, Phys. Rev. D **51**, 4819 (1995).

[24] S. Acharya *et al.* (ALICE Collaboration), Measurement of the cross sections of Ξ_c^0 and Ξ_c^+ baryons and of the branching-fraction ratio BR($\Xi_c^0 \to \Xi^- e^+ \nu_e$)/BR($\Xi_c^0 \to \Xi^- \pi^+$) in pp collisions at 13 TeV, Phys. Rev. Lett. **127**, 272001 (2021).

[25] S. Acharya *et al.* (ALICE Collaboration), Λ_c^+ production and baryon-to-meson ratios in pp and p–Pb collisions at $\sqrt{s_{NN}} = 5.02$ TeV at the LHC, Phys. Rev. Lett. **127**, 202301 (2021).

[26] S. Acharya *et al.* (ALICE Collaboration), Λ_c^+ production in pp and in p–Pb collisions at $\sqrt{s_{NN}} = 5.02$ TeV, Phys. Rev. C **104**, 054905 (2021).

[27] S. Acharya *et al.* (ALICE Collaboration), Measurement of prompt D^0, Λ_c^+, and $\Sigma_c^{0,++}(2455)$ production in proton–proton collisions at $\sqrt{s} = 13$ TeV, Phys. Rev. Lett. **128**, 012001 (2022).

[28] S. Acharya *et al.* (ALICE Collaboration), First measurement of $\Omega c0$ production in pp collisions at s = 13 TeV, Phys. Lett. B **846**, 137625 (2023).

[29] A. M. Sirunyan *et al.* (CMS Collaboration), Production of Λ_c^+ baryons in proton-proton and lead-lead collisions at $\sqrt{s_{NN}} = 5.02$ TeV, Phys. Lett. B **803**, 135328 (2020).

[30] S. Acharya *et al.* (ALICE Collaboration), Charm-quark fragmentation fractions and production cross section at midrapidity in pp collisions at the LHC, Phys. Rev. D **105**, L011103 (2022).

[31] S. Acharya *et al.* (ALICE Collaboration), First measurement of $\Lambda c+$ production down to pT = 0 in pp and p-Pb collisions at sNN = 5.02 TeV, Phys. Rev. C **107**, 064901 (2023).

[32] S. Acharya *et al.* (ALICE Collaboration), Measurement of the production cross section of prompt Ξ_c^0 baryons at midrapidity in pp collisions at $\sqrt{s} = 5.02$ TeV, J. High Energy Phys. 10 (2021) 159.

[33] J. Song, H.-H. Li, and F.-L. Shao, New feature of low p_T charm quark hadronization in pp collisions at $\sqrt{s} = 7$ TeV, Eur. Phys. J. C **78**, 344 (2018).

[34] V. Minissale, S. Plumari, and V. Greco, Charm hadrons in pp collisions at LHC energy within a coalescence plus fragmentation approach, Phys. Lett. B **821**, 136622 (2021).

[35] D. Ebert, R. N. Faustov, and V. O. Galkin, Spectroscopy and Regge trajectories of heavy baryons in the relativistic quark-diquark picture, Phys. Rev. D **84**, 014025 (2011).

[36] M. He and R. Rapp, Charm-baryon production in proton-proton collisions, Phys. Lett. B **795**, 117 (2019).

[37] J. R. Christiansen and P. Z. Skands, String formation beyond leading colour, J. High Energy Phys. 08 (2015) 003.

[38] R. Aaij *et al.* (LHCb Collaboration), Study of the production of Λ_b^0 and $\bar{B}^0$ hadrons in pp collisions and first measurement of the $\Lambda_b^0 \to J/\psi p K^-$ branching fraction, Chin. Phys. C **40**, 011001 (2016).

[39] R. Aaij *et al.* (LHCb Collaboration), Measurement of b hadron fractions in 13 TeV pp collisions, Phys. Rev. D **100**, 031102 (2019).

[40] R. Aaij *et al.* (LHCb Collaboration), Prompt charm production in pp collisions at $\sqrt{s} = 7$ TeV, Nucl. Phys. **B871,** 1 (2013).

[41] R. Aaij *et al.* (LHCb Collaboration), Prompt Λ_c^+ production in pPb collisions at $\sqrt{s_{NN}} = 5.02$ TeV, J. High Energy Phys. 02 (2019) 102.

[42] A. M. Sirunyan *et al.* (CMS Collaboration), Measurement of the $B^\pm$ meson nuclear modification factor in Pb-Pb collisions at $\sqrt{s_{NN}} = 5.02$ TeV, Phys. Rev. Lett. **119,** 152301 (2017).

[43] A. M. Sirunyan *et al.* (CMS Collaboration), Measurement of B_s^0 meson production in pp and PbPb collisions at $\sqrt{s_{NN}} = 5.02$ TeV, Phys. Lett. B **796,** 168 (2019).

[44] G. Aad *et al.* (ATLAS Collaboration), Measurement of the differential cross-section of B^+ meson production in pp collisions at $\sqrt{s} = 7$ TeV at ATLAS, J. High Energy Phys. 10 (2013) 042.

[45] V. Khachatryan *et al.* (CMS Collaboration), Measurement of the B^+ production cross section in pp collisions at $\sqrt{s} = 7$ TeV, Phys. Rev. Lett. **106,** 112001 (2011).

[46] S. Chatrchyan *et al.* (CMS Collaboration), Measurement of the strange B meson production cross section with J/Psi ϕ decays in pp collisions at $\sqrt{s} = 7$ TeV, Phys. Rev. D **84,** 052008 (2011).

[47] S. Chatrchyan *et al.* (CMS Collaboration), Measurement of the B^0 production cross section in pp collisions at $\sqrt{s} = 7$ TeV, Phys. Rev. Lett. **106,** 252001 (2011).

[48] S. Chatrchyan *et al.* (CMS Collaboration), Measurement of the Λ_b cross section and the $\bar{\Lambda}_b$ to Λ_b ratio with $J/\Psi\Lambda$ decays in pp collisions at $\sqrt{s} = 7$ TeV, Phys. Lett. B **714,** 136 (2012).

[49] M. He and R. Rapp, Bottom hadro-chemistry in high-energy hadronic collisions, Phys. Rev. Lett. **131,** 012301 (2023).

[50] T. Sjöstrand, S. Ask, J. R. Christiansen, R. Corke, N. Desai, P. Ilten, S. Mrenna, S. Prestel, C. O. Rasmussen, and P. Z. Skands, An Introduction to PYTHIA8.2, Comput. Phys. Commun. **191,** 159 (2015).

[51] B. Abelev *et al.* (ALICE Collaboration), Performance of the ALICE experiment at the CERN LHC, Int. J. Mod. Phys. A **29,** 1430044 (2014).

[52] K. Aamodt *et al.* (ALICE Collaboration), The ALICE experiment at the CERN LHC, J. Instrum. **3,** S08002 (2008).

[53] S. Acharya *et al.* (ALICE Collaboration), ALICE 2016-2017-2018 luminosity determination for pp collisions at $\sqrt{s} = 13$ TeV, Report No. ALICE-PUBLIC-2021-005, 2021.

[54] R. L. Workman *et al.* (Particle Data Group Collaboration), Review of particle physics, Prog. Theor. Exp. Phys. **2022,** 083C01 (2022).

[55] I. Kisel, I. Kulakov, and M. Zyzak, Standalone first level event selection package for the CBM experiment, IEEE Trans. Nucl. Sci. **60,** 3703 (2013).

[56] T. Chen and C. Guestrin, Xgboost: A scalable tree boosting system, *Proceedings of the 22nd ACM SIGKDD International Conference on Knowledge Discovery and Data Mining* (2016), p. 785; arXiv:1603.02754.

[57] L. Barioglio, F. Catalano, M. Concas, P. Fecchio, F. Grosa, F. Mazzaschi, and M. Puccio, hipe4 ml/hipe4ml (2021), 10.5281/zenodo.5070132.

[58] P. Skands, S. Carrazza, and J. Rojo, Tuning PYTHIA8.1: The Monash 2013 Tune, Eur. Phys. J. C **74,** 3024 (2014).

[59] R. Brun, F. Carminati, and S. Giani, CERN Program Library Long Write-up, W5013 GEANT Detector Description and Simulation Tool, Technical Report No. CERN-W-5013, 1994.

[60] S. Acharya *et al.* (ALICE Collaboration), Observation of a multiplicity dependence in the p_T-differential charm baryon-to-meson ratios in proton-proton collisions at $\sqrt{s} = 13$ TeV, Phys. Lett. B **829,** 137065 (2022).

[61] R. L. Workman *et al.* (Particle Data Group Collaboration), Review of particle physics, Prog. Theor. Exp. Phys. **2022,** 083C01 (2022).

[62] S. Alioli, P. Nason, C. Oleari, and E. Re, A general framework for implementing NLO calculations in shower Monte Carlo programs: The POWHEG BOX, J. High Energy Phys. 06 (2010) 043.

[63] H.-L. Lai, M. Guzzi, J. Huston, Z. Li, P. M. Nadolsky, J. Pumplin, and C. P. Yuan, New parton distributions for collider physics, Phys. Rev. D **82,** 074024 (2010).

[64] S. Dulat, T.-J. Hou, J. Gao, M. Guzzi, J. Huston, P. Nadolsky, J. Pumplin, C. Schmidt, D. Stump, and C. P. Yuan, New parton distribution functions from a global analysis of quantum chromodynamics, Phys. Rev. D **93,** 033006 (2016).

[65] S. Acharya *et al.* (ALICE Collaboration), Dielectron and heavy-quark production in inelastic and high-multiplicity proton–proton collisions at $\sqrt{s} = 13$ TeV, Phys. Lett. B **788,** 505 (2019).

[66] S. Acharya *et al.* (ALICE Collaboration), Dielectron production in proton-proton and proton-lead collisions at $\sqrt{s_{NN}} = 5.02$ TeV, Phys. Rev. C **102,** 055204 (2020).

[67] S. Acharya *et al.* (ALICE Collaboration), Production of light-flavor hadrons in pp collisions at $\sqrt{s} = 7$ and $\sqrt{s} = 13$ TeV, Eur. Phys. J. C **81,** 256 (2021).

[68] L. Gladilin, Fragmentation fractions of c and b quarks into charmed hadrons at LEP, Eur. Phys. J. C **75,** 19 (2015).

S. Acharya,[128] D. Adamová,[87] G. Aglieri Rinella,[33] M. Agnello,[30] N. Agrawal,[52] Z. Ahammed,[136] S. Ahmad,[16] S. U. Ahn,[72] I. Ahuja,[38] A. Akindinov,[142] M. Al-Turany,[98] D. Aleksandrov,[142] B. Alessandro,[57] H. M. Alfanda,[6] R. Alfaro Molina,[68] B. Ali,[16] A. Alici,[26a,26b] N. Alizadehvandchali,[117] A. Alkin,[33] J. Alme,[21] G. Alocco,[53] T. Alt,[65] A. R. Altamura,[51] I. Altsybeev,[96] M. N. Anaam,[6] C. Andrei,[46] N. Andreou,[116] A. Andronic,[127] V. Anguelov,[95] F. Antinori,[55] P. Antonioli,[52] N. Apadula,[75] L. Aphecetche,[104] H. Appelshäuser,[65] C. Arata,[74] S. Arcelli,[26a,26b] M. Aresti,[23a,23b] R. Arnaldi,[57] J. G. M. C. A. Arneiro,[111] I. C. Arsene,[20] M. Arslandok,[139] A. Augustinus,[33] R. Averbeck,[98] M. D. Azmi,[16] H. Baba,[125] A. Badalà,[54] J. Bae,[105] Y. W. Baek,[41] X. Bai,[121] R. Bailhache,[65] Y. Bailung,[49] A. Balbino,[30] A. Baldisseri,[131] B. Balis,[2]

D. Banerjee,[4a,4b] Z. Banoo,[92] R. Barbera,[27a,27b] F. Barile,[32a,32b] L. Barioglio,[96] M. Barlou,[79] B. Barman,[42] G. G. Barnaföldi,[47] L. S. Barnby,[86] V. Barret,[128] L. Barreto,[111] C. Bartels,[120] K. Barth,[33] E. Bartsch,[65] N. Bastid,[128] S. Basu,[76] G. Batigne,[104] D. Battistini,[96] B. Batyunya,[143] D. Bauri,[48] J. L. Bazo Alba,[102] I. G. Bearden,[84] C. Beattie,[139] P. Becht,[98] D. Behera,[49] I. Belikov,[130] A. D. C. Bell Hechavarria,[127] F. Bellini,[26a,26b] R. Bellwied,[117] S. Belokurova,[142] G. Bencedi,[47] S. Beole,[25a,25b] Y. Berdnikov,[142] A. Berdnikova,[95] L. Bergmann,[95] M. G. Besoiu,[64] L. Betev,[33] P. P. Bhaduri,[136] A. Bhasin,[92] M. A. Bhat,[4a,4b] B. Bhattacharjee,[42] L. Bianchi,[25a,25b] N. Bianchi,[50] J. Bielčík,[36] J. Bielčíková,[87] J. Biernat,[108] A. P. Bigot,[130] A. Bilandzic,[96] G. Biro,[47] S. Biswas,[4a,4b] N. Bize,[104] J. T. Blair,[109] D. Blau,[142] M. B. Blidaru,[98] N. Bluhme,[39] C. Blume,[65] G. Boca,[22,56] F. Bock,[88] T. Bodova,[21] A. Bogdanov,[142] S. Boi,[23a,23b] J. Bok,[59] L. Boldizsár,[47] M. Bombara,[38] P. M. Bond,[33] G. Bonomi,[56,135] H. Borel,[131] A. Borissov,[142] A. G. Borquez Carcamo,[95] H. Bossi,[139] E. Botta,[25a,25b] Y. E. M. Bouziani,[65] L. Bratrud,[65] P. Braun-Munzinger,[98] M. Bregant,[111] M. Broz,[36] G. E. Bruno,[32a,32b,97] M. D. Buckland,[24a,24b] D. Budnikov,[142] H. Buesching,[65] S. Bufalino,[30] P. Buhler,[103] N. Burmasov,[142] Z. Buthelezi,[69,124] A. Bylinkin,[21] S. A. Bysiak,[108] M. Cai,[6] H. Caines,[139] A. Caliva,[29a,29b] E. Calvo Villar,[102] J. M. M. Camacho,[110] P. Camerini,[24a,24b] F. D. M. Canedo,[111] M. Carabas,[114] A. A. Carballo,[33] F. Carnesecchi,[33] R. Caron,[129] L. A. D. Carvalho,[111] J. Castillo Castellanos,[131] F. Catalano,[25a,25b,33] C. Ceballos Sanchez,[143] I. Chakaberia,[75] P. Chakraborty,[48] S. Chandra,[136] S. Chapeland,[33] M. Chartier,[120] S. Chattopadhyay,[136] S. Chattopadhyay,[100] T. G. Chavez,[45] T. Cheng,[6,98] C. Cheshkov,[129] B. Cheynis,[129] V. Chibante Barroso,[33] D. D. Chinellato,[112] E. S. Chizzali,[96,‡] J. Cho,[59] S. Cho,[59] P. Chochula,[33] D. Choudhury,[42] P. Christakoglou,[85] C. H. Christensen,[84] P. Christiansen,[76] T. Chujo,[126] M. Ciacco,[30] C. Cicalo,[53] F. Cindolo,[52] M. R. Ciupek,[98] G. Clai,[52,§] F. Colamaria,[51] J. S. Colburn,[101] D. Colella,[32a,32b,97] M. Colocci,[26a,26b] M. Concas,[57,‖] G. Conesa Balbastre,[74] Z. Conesa del Valle,[132] G. Contin,[24a,24b] J. G. Contreras,[36] M. L. Coquet,[131] P. Cortese,[57,134] M. R. Cosentino,[113] F. Costa,[33] S. Costanza,[22,56] C. Cot,[132] J. Crkovská,[95] P. Crochet,[128] R. Cruz-Torres,[75] P. Cui,[6] A. Dainese,[55] M. C. Danisch,[95] A. Danu,[64] P. Das,[81] P. Das,[4a,4b] S. Das,[4a,4b] A. R. Dash,[127] S. Dash,[48] R. M. H. David,[45] A. De Caro,[29a,29b] G. de Cataldo,[51] J. de Cuveland,[39] A. De Falco,[23a,23b] D. De Gruttola,[29a,29b] N. De Marco,[57] C. De Martin,[24a,24b] S. De Pasquale,[29a,29b] R. Deb,[135] R. Del Grande,[96] L. Dello Stritto,[29a,29b] W. Deng,[6] P. Dhankher,[19] D. Di Bari,[32a,32b] A. Di Mauro,[33] B. Diab,[131] R. A. Diaz,[7,143] T. Dietel,[115] Y. Ding,[6] R. Divià,[33] D. U. Dixit,[19] Ø. Djuvsland,[21] U. Dmitrieva,[142] A. Dobrin,[64] B. Dönigus,[65] J. M. Dubinski,[137] A. Dubla,[98] S. Dudi,[91] P. Dupieux,[128] M. Durkac,[107] N. Dzalaiova,[13] T. M. Eder,[127] R. J. Ehlers,[75] F. Eisenhut,[65] R. Ejima,[93] D. Elia,[51] B. Erazmus,[104] F. Ercolessi,[26a,26b] F. Erhardt,[90] M. R. Ersdal,[21] B. Espagnon,[132] G. Eulisse,[33] D. Evans,[101] S. Evdokimov,[142] L. Fabbietti,[96] M. Faggin,[28a,28b] J. Faivre,[74] F. Fan,[6] W. Fan,[75] A. Fantoni,[50] M. Fasel,[88] P. Fecchio,[30] A. Feliciello,[57] G. Feofilov,[142] A. Fernández Téllez,[45] L. Ferrandi,[111] M. B. Ferrer,[33] A. Ferrero,[131] C. Ferrero,[57] A. Ferretti,[25a,25b] V. J. G. Feuillard,[95] V. Filova,[36] D. Finogeev,[142] F. M. Fionda,[53] F. Flor,[117] A. N. Flores,[109] S. Foertsch,[69] I. Fokin,[95] S. Fokin,[142] E. Fragiacomo,[58] E. Frajna,[47] U. Fuchs,[33] N. Funicello,[29a,29b] C. Furget,[74] A. Furs,[142] T. Fusayasu,[99] J. J. Gaardhøje,[84] M. Gagliardi,[25a,25b] A. M. Gago,[102] T. Gahlaut,[48] C. D. Galvan,[110] D. R. Gangadharan,[117] P. Ganoti,[79] C. Garabatos,[98] A. T. Garcia,[132] J. R. A. Garcia,[45] E. Garcia-Solis,[9] C. Gargiulo,[33] K. Garner,[127] P. Gasik,[98] A. Gautam,[119] M. B. Gay Ducati,[67] M. Germain,[104] A. Ghimouz,[126] C. Ghosh,[136] M. Giacalone,[52] G. Gioachin,[30] P. Giubellino,[57,98] P. Giubilato,[28a,28b] A. M. C. Glaenzer,[131] P. Glässel,[95] E. Glimos,[123] D. J. Q. Goh,[77] V. Gonzalez,[138] M. Gorgon,[2] K. Goswami,[49] S. Gotovac,[34] V. Grabski,[68] L. K. Graczykowski,[137] E. Grecka,[87] A. Grelli,[60] C. Grigoras,[33] V. Grigoriev,[142] S. Grigoryan,[1,143] F. Grosa,[33] J. F. Grosse-Oetringhaus,[33] R. Grosso,[98] D. Grund,[36] G. G. Guardiano,[112] R. Guernane,[74] M. Guilbaud,[104] K. Gulbrandsen,[84] T. Gündem,[65] T. Gunji,[125] W. Guo,[6] A. Gupta,[92] R. Gupta,[92] R. Gupta,[49] S. P. Guzman,[45] K. Gwizdziel,[137] L. Gyulai,[47] C. Hadjidakis,[132] F. U. Haider,[92] H. Hamagaki,[77] A. Hamdi,[75] Y. Han,[140] B. G. Hanley,[138] R. Hannigan,[109] J. Hansen,[76] M. R. Haque,[137] J. W. Harris,[139] A. Harton,[9] H. Hassan,[88] D. Hatzifotiadou,[52] P. Hauer,[43] L. B. Havener,[139] S. T. Heckel,[96] E. Hellbär,[98] H. Helstrup,[35] M. Hemmer,[65] T. Herman,[36] G. Herrera Corral,[8] F. Herrmann,[127] S. Herrmann,[129] K. F. Hetland,[35] B. Heybeck,[65] H. Hillemanns,[33] B. Hippolyte,[130] F. W. Hoffmann,[71] B. Hofman,[60] G. H. Hong,[140] M. Horst,[96] A. Horzyk,[2] Y. Hou,[6] P. Hristov,[33] C. Hughes,[123] P. Huhn,[65] L. M. Huhta,[118] T. J. Humanic,[89] A. Hutson,[117] D. Hutter,[39] R. Ilkaev,[142] H. Ilyas,[14] M. Inaba,[126] G. M. Innocenti,[33] M. Ippolitov,[142] A. Isakov,[85,87] T. Isidori,[119] M. S. Islam,[100] M. Ivanov,[13] M. Ivanov,[98] V. Ivanov,[142] K. E. Iversen,[76] M. Jablonski,[2] B. Jacak,[75] N. Jacazio,[26a,26b] P. M. Jacobs,[75] S. Jadlovska,[107] J. Jadlovsky,[107] S. Jaelani,[83] C. Jahnke,[112] M. J. Jakubowska,[137] M. A. Janik,[137] T. Janson,[71] S. Ji,[17] S. Jia,[10] A. A. P. Jimenez,[66] F. Jonas,[88] D. M. Jones,[120] J. M. Jowett,[33,98] J. Jung,[65] M. Jung,[65] A. Junique,[33] A. Jusko,[101] M. J. Kabus,[33,137] J. Kaewjai,[106] P. Kalinak,[61] A. S. Kalteyer,[98] A. Kalweit,[33] V. Kaplin,[142] A. Karasu Uysal,[73] D. Karatovic,[90] O. Karavichev,[142] T. Karavicheva,[142] P. Karczmarczyk,[137] E. Karpechev,[142] U. Kebschull,[71] R. Keidel,[141] D. L. D. Keijdener,[60] M. Keil,[33]

B. Ketzer,[43] S. S. Khade,[49] A. M. Khan,[6,121] S. Khan,[16] A. Khanzadeev,[142] Y. Kharlov,[142] A. Khatun,[119] A. Khuntia,[36] B. Kileng,[35] B. Kim,[105] C. Kim,[17] D. J. Kim,[118] E. J. Kim,[70] J. Kim,[140] J. S. Kim,[41] J. Kim,[59] J. Kim,[70] M. Kim,[19] S. Kim,[18] T. Kim,[140] K. Kimura,[93] S. Kirsch,[65] I. Kisel,[39] S. Kiselev,[142] A. Kisiel,[137] J. P. Kitowski,[2] J. L. Klay,[5] J. Klein,[33] S. Klein,[75] C. Klein-Bösing,[127] M. Kleiner,[65] T. Klemenz,[96] A. Kluge,[33] A. G. Knospe,[117] C. Kobdaj,[106] T. Kollegger,[98] A. Kondratyev,[143] N. Kondratyeva,[142] E. Kondratyuk,[142] J. Konig,[65] S. A. Konigstorfer,[96] P. J. Konopka,[33] G. Kornakov,[137] M. Korwieser,[96] S. D. Koryciak,[2] A. Kotliarov,[87] V. Kovalenko,[142] M. Kowalski,[108] V. Kozhuharov,[37] I. Králik,[61] A. Kravčáková,[38] L. Krcal,[33,39] M. Krivda,[61,101] F. Krizek,[87] K. Krizkova Gajdosova,[33] M. Kroesen,[95] M. Krüger,[65] D. M. Krupova,[36] E. Kryshen,[142] V. Kučera,[59] C. Kuhn,[130] P. G. Kuijer,[85] T. Kumaoka,[126] D. Kumar,[136] L. Kumar,[91] N. Kumar,[91] S. Kumar,[32a,32b] S. Kundu,[33] P. Kurashvili,[80] A. Kurepin,[142] A. B. Kurepin,[142] A. Kuryakin,[142] S. Kushpil,[87] M. J. Kweon,[59] Y. Kwon,[140] S. L. La Pointe,[39] P. La Rocca,[27a,27b] A. Lakrathok,[106] M. Lamanna,[33] A. R. Landou,[74,116] R. Langoy,[122] P. Larionov,[33] E. Laudi,[33] L. Lautner,[33,96] R. Lavicka,[103] R. Lea,[56,135] H. Lee,[105] I. Legrand,[46] G. Legras,[127] J. Lehrbach,[39] T. M. Lelek,[2] R. C. Lemmon,[86] I. León Monzón,[110] M. M. Lesch,[96] E. D. Lesser,[19] P. Lévai,[47] X. Li,[10] X. L. Li,[6] J. Lien,[122] R. Lietava,[101] I. Likmeta,[117] B. Lim,[25a,25b] S. H. Lim,[17] V. Lindenstruth,[39] A. Lindner,[46] C. Lippmann,[98] A. Liu,[19] D. H. Liu,[6] J. Liu,[120] G. S. S. Liveraro,[112] I. M. Lofnes,[21] C. Loizides,[88] S. Lokos,[108] J. Lomker,[60] P. Loncar,[34] X. Lopez,[128] E. López Torres,[7] P. Lu,[98,121] J. R. Luhder,[127] M. Lunardon,[28a,28b] G. Luparello,[58] Y. G. Ma,[40] M. Mager,[33] A. Maire,[130] M. V. Makariev,[37] M. Malaev,[142] G. Malfattore,[26a,26b] N. M. Malik,[92] Q. W. Malik,[20] S. K. Malik,[92] L. Malinina,[143,†,¶] D. Mallick,[81,132] N. Mallick,[49] G. Mandaglio,[31,54] S. K. Mandal,[80] V. Manko,[142] F. Manso,[128] V. Manzari,[51] Y. Mao,[6] R. W. Marcjan,[2] G. V. Margagliotti,[24a,24b] A. Margotti,[52] A. Marín,[98] C. Markert,[109] P. Martinengo,[33] M. I. Martínez,[45] G. Martínez García,[104] M. P. P. Martins,[111] S. Masciocchi,[98] M. Masera,[25a,25b] A. Masoni,[53] L. Massacrier,[132] O. Massen,[60] A. Mastroserio,[51,133] O. Matonoha,[76] S. Mattiazzo,[28a,28b] P. F. T. Matuoka,[111] A. Matyja,[108] C. Mayer,[108] A. L. Mazuecos,[33] F. Mazzaschi,[25a,25b] M. Mazzilli,[33] J. E. Mdhluli,[124] A. F. Mechler,[65] Y. Melikyan,[44] A. Menchaca-Rocha,[68] E. Meninno,[103] A. S. Menon,[117] M. Meres,[13] S. Mhlanga,[69,115] Y. Miake,[126] L. Micheletti,[33] L. C. Migliorin,[129] D. L. Mihaylov,[96] K. Mikhaylov,[142,143] A. N. Mishra,[47] D. Miśkowiec,[98] A. Modak,[4a,4b] A. P. Mohanty,[60] B. Mohanty,[81] M. Mohisin Khan,[16,**] M. A. Molander,[44] S. Monira,[137] Z. Moravcova,[84] C. Mordasini,[118] D. A. Moreira De Godoy,[127] I. Morozov,[142] A. Morsch,[33] T. Mrnjavac,[33] V. Muccifora,[50] S. Muhuri,[136] J. D. Mulligan,[75] A. Mulliri,[23a,23b] M. G. Munhoz,[111] R. H. Munzer,[65] H. Murakami,[125] S. Murray,[115] L. Musa,[33] J. Musinsky,[61] J. W. Myrcha,[137] B. Naik,[124] A. I. Nambrath,[19] B. K. Nandi,[48] R. Nania,[52] E. Nappi,[51] A. F. Nassirpour,[18,76] A. Nath,[95] C. Nattrass,[123] M. N. Naydenov,[37] A. Neagu,[20] A. Negru,[114] L. Nellen,[66] R. Nepeivoda,[76] S. Nese,[20] G. Neskovic,[39] N. Nicassio,[51] B. S. Nielsen,[84] E. G. Nielsen,[84] S. Nikolaev,[142] S. Nikulin,[142] V. Nikulin,[142] F. Noferini,[52] S. Noh,[12] P. Nomokonov,[143] J. Norman,[120] N. Novitzky,[126] P. Nowakowski,[137] A. Nyanin,[142] J. Nystrand,[21] M. Ogino,[77] S. Oh,[18] A. Ohlson,[76] V. A. Okorokov,[142] J. Oleniacz,[137] A. C. Oliveira Da Silva,[123] M. H. Oliver,[139] A. Onnerstad,[118] C. Oppedisano,[57] A. Ortiz Velasquez,[66] J. Otwinowski,[108] M. Oya,[93] K. Oyama,[77] Y. Pachmayer,[95] S. Padhan,[48] D. Pagano,[56,135] G. Paić,[66] A. Palasciano,[51] S. Panebianco,[131] H. Park,[126] H. Park,[105] J. Park,[59] J. E. Parkkila,[33] Y. Patley,[48] R. N. Patra,[92] B. Paul,[23a,23b] H. Pei,[6] T. Peitzmann,[60] X. Peng,[11] M. Pennisi,[25a,25b] S. Perciballi,[25a,25b] D. Peresunko,[142] G. M. Perez,[7] Y. Pestov,[142] V. Petrov,[142] M. Petrovici,[46] R. P. Pezzi,[67,104] S. Piano,[58] M. Pikna,[13] P. Pillot,[104] O. Pinazza,[33,52] L. Pinsky,[117] C. Pinto,[96] S. Pisano,[50] M. Płoskoń,[75] M. Planinic,[90] F. Pliquett,[65] M. G. Poghosyan,[88] B. Polichtchouk,[142] S. Politano,[30] N. Poljak,[90] A. Pop,[46] S. Porteboeuf-Houssais,[128] V. Pozdniakov,[143] I. Y. Pozos,[45] K. K. Pradhan,[49] S. K. Prasad,[4a,4b] S. Prasad,[49] R. Preghenella,[52] F. Prino,[57] C. A. Pruneau,[138] I. Pshenichnov,[142] M. Puccio,[33] S. Pucillo,[25a,25b] Z. Pugelova,[107] S. Qiu,[85] L. Quaglia,[25a,25b] R. E. Quishpe,[117] S. Ragoni,[15] A. Rai,[139] A. Rakotozafindrabe,[131] L. Ramello,[57,134] F. Rami,[130] S. A. R. Ramirez,[45] T. A. Rancien,[74] M. Rasa,[27a,27b] S. S. Räsänen,[44] R. Rath,[52] M. P. Rauch,[21] I. Ravasenga,[85] K. F. Read,[88,123] C. Reckziegel,[113] A. R. Redelbach,[39] K. Redlich,[80,††] C. A. Reetz,[98] A. Rehman,[21] F. Reidt,[33] H. A. Reme-Ness,[35] Z. Rescakova,[38] K. Reygers,[95] A. Riabov,[142] V. Riabov,[142] R. Ricci,[29a,29b] M. Richter,[20] A. A. Riedel,[96] W. Riegler,[33] A. G. Riffero,[25a,25b] C. Ristea,[64] M. V. Rodriguez,[33] M. Rodríguez Cahuantzi,[45] K. Røed,[20] R. Rogalev,[142] E. Rogochaya,[143] T. S. Rogoschinski,[65] D. Rohr,[33] D. Röhrich,[21] P. F. Rojas,[45] S. Rojas Torres,[36] P. S. Rokita,[137] G. Romanenko,[26a,26b] F. Ronchetti,[50] A. Rosano,[31,54] E. D. Rosas,[66] K. Roslon,[137] A. Rossi,[55] A. Roy,[49] S. Roy,[48] N. Rubini,[26a,26b] D. Ruggiano,[137] R. Rui,[24a,24b] P. G. Russek,[2] R. Russo,[85] A. Rustamov,[82] E. Ryabinkin,[142] Y. Ryabov,[142] A. Rybicki,[108] H. Rytkonen,[118] J. Ryu,[17] W. Rzesa,[137] O. A. M. Saarimaki,[44] S. Sadhu,[32a,32b] S. Sadovsky,[142] J. Saetre,[21] K. Šafařík,[36] P. Saha,[42] S. K. Saha,[4a,4b] S. Saha,[81] B. Sahoo,[48] B. Sahoo,[49] R. Sahoo,[49] S. Sahoo,[62] D. Sahu,[49] P. K. Sahu,[62] J. Saini,[136] K. Sajdakova,[38] S. Sakai,[126] M. P. Salvan,[98] S. Sambyal,[92] D. Samitz,[103] I. Sanna,[33,96]

T. B. Saramela,[111] P. Sarma,[42] V. Sarritzu,[23a,23b] V. M. Sarti,[96] M. H. P. Sas,[139] J. Schambach,[88] H. S. Scheid,[65] C. Schiaua,[46] R. Schicker,[95] A. Schmah,[98] C. Schmidt,[98] H. R. Schmidt,[94] M. O. Schmidt,[33] M. Schmidt,[94] N. V. Schmidt,[88] A. R. Schmier,[123] R. Schotter,[130] A. Schröter,[39] J. Schukraft,[33] K. Schweda,[98] G. Scioli,[26a,26b] E. Scomparin,[57] J. E. Seger,[15] Y. Sekiguchi,[125] D. Sekihata,[125] M. Selina,[85] I. Selyuzhenkov,[98] S. Senyukov,[130] J. J. Seo,[59,95] D. Serebryakov,[142] L. Šerkšnytė,[96] A. Sevcenco,[64] T. J. Shaba,[69] A. Shabetai,[104] R. Shahoyan,[33] A. Shangaraev,[142] A. Sharma,[91] B. Sharma,[92] D. Sharma,[48] H. Sharma,[55,108] M. Sharma,[92] S. Sharma,[77] S. Sharma,[92] U. Sharma,[92] A. Shatat,[132] O. Sheibani,[117] K. Shigaki,[93] M. Shimomura,[78] J. Shin,[12] S. Shirinkin,[142] Q. Shou,[40] Y. Sibiriak,[142] S. Siddhanta,[53] T. Siemiarczuk,[80] T. F. Silva,[111] D. Silvermyr,[76] T. Simantathammakul,[106] R. Simeonov,[37] B. Singh,[92] B. Singh,[96] K. Singh,[49] R. Singh,[81] R. Singh,[92] R. Singh,[49] S. Singh,[16] V. K. Singh,[136] V. Singhal,[136] T. Sinha,[100] B. Sitar,[13] M. Sitta,[57,134] T. B. Skaali,[20] G. Skorodumovs,[95] M. Slupecki,[44] N. Smirnov,[139] R. J. M. Snellings,[60] E. H. Solheim,[20] J. Song,[117] A. Songmoolnak,[106] C. Sonnabend,[33,98] F. Soramel,[28a,28b] A. B. Soto-hernandez,[89] R. Spijkers,[85] I. Sputowska,[108] J. Staa,[76] J. Stachel,[95] I. Stan,[64] P. J. Steffanic,[123] S. F. Stiefelmaier,[95] D. Stocco,[104] I. Storehaug,[20] P. Stratmann,[127] S. Strazzi,[26a,26b] A. Sturniolo,[31,54] C. P. Stylianidis,[85] A. A. P. Suaide,[111] C. Suire,[132] M. Sukhanov,[142] M. Suljic,[33] R. Sultanov,[142] V. Sumberia,[92] S. Sumowidagdo,[83] S. Swain,[62] I. Szarka,[13] M. Szymkowski,[137] S. F. Taghavi,[96] G. Taillepied,[98] J. Takahashi,[112] G. J. Tambave,[81] S. Tang,[6] Z. Tang,[121] J. D. Tapia Takaki,[119] N. Tapus,[114] L. A. Tarasovicova,[127] M. G. Tarzila,[46] G. F. Tassielli,[32a,32b] A. Tauro,[33] G. Tejeda Muñoz,[45] A. Telesca,[33] L. Terlizzi,[25a,25b] C. Terrevoli,[117] S. Thakur,[4a,4b] D. Thomas,[109] A. Tikhonov,[142] A. R. Timmins,[117] M. Tkacik,[107] T. Tkacik,[107] A. Toia,[65] R. Tokumoto,[93] K. Tomohiro,[93] N. Topilskaya,[142] M. Toppi,[50] T. Tork,[132] V. V. Torres,[104] A. G. Torres Ramos,[32a,32b] A. Trifiró,[31,54] A. S. Triolo,[31,33,54] S. Tripathy,[52] T. Tripathy,[48] S. Trogolo,[33] V. Trubnikov,[3] W. H. Trzaska,[118] T. P. Trzcinski,[137] A. Tumkin,[142] R. Turrisi,[55] T. S. Tveter,[20] K. Ullaland,[21] B. Ulukutlu,[96] A. Uras,[129] G. L. Usai,[23a,23b] M. Vala,[38] N. Valle,[22] L. V. R. van Doremalen,[60] M. van Leeuwen,[85] C. A. van Veen,[95] R. J. G. van Weelden,[85] P. Vande Vyvre,[33] D. Varga,[47] Z. Varga,[47] M. Vasileiou,[79] A. Vasiliev,[142] O. Vázquez Doce,[50] O. Vazquez Rueda,[117] V. Vechernin,[142] E. Vercellin,[25a,25b] S. Vergara Limón,[45] R. Verma,[48] L. Vermunt,[98] R. Vértesi,[47] M. Verweij,[60] L. Vickovic,[34] Z. Vilakazi,[124] O. Villalobos Baillie,[101] A. Villani,[24a,24b] G. Vino,[51] A. Vinogradov,[142] T. Virgili,[29a,29b] M. M. O. Virta,[118] V. Vislavicius,[76] A. Vodopyanov,[143] B. Volkel,[33] M. A. Völkl,[95] K. Voloshin,[142] S. A. Voloshin,[138] G. Volpe,[32a,32b] B. von Haller,[33] I. Vorobyev,[96] N. Vozniuk,[142] J. Vrláková,[38] J. Wan,[40] C. Wang,[40] D. Wang,[40] Y. Wang,[40] Y. Wang,[6] A. Wegrzynek,[33] F. T. Weiglhofer,[39] S. C. Wenzel,[33] J. P. Wessels,[127] S. L. Weyhmiller,[139] J. Wiechula,[65] J. Wikne,[20] G. Wilk,[80] J. Wilkinson,[98] G. A. Willems,[127] B. Windelband,[95] M. Winn,[131] J. R. Wright,[109] W. Wu,[40] Y. Wu,[121] R. Xu,[6] A. Yadav,[43] A. K. Yadav,[136] S. Yalcin,[73] Y. Yamaguchi,[93] S. Yang,[21] S. Yano,[93] Z. Yin,[6] I.-K. Yoo,[17] J. H. Yoon,[59] H. Yu,[12] S. Yuan,[21] A. Yuncu,[95] V. Zaccolo,[24a,24b] C. Zampolli,[33] F. Zanone,[95] N. Zardoshti,[33] A. Zarochentsev,[142] P. Závada,[63] N. Zaviyalov,[142] M. Zhalov,[142] B. Zhang,[6] C. Zhang,[131] L. Zhang,[40] S. Zhang,[40] X. Zhang,[6] Y. Zhang,[121] Z. Zhang,[6] M. Zhao,[10] V. Zherebchevskii,[142] Y. Zhi,[10] D. Zhou,[6] Y. Zhou,[84] J. Zhu,[6,98] Y. Zhu,[6] S. C. Zugravel,[57] and N. Zurlo[56,135]

(ALICE Collaboration)

[1]*A.I. Alikhanyan National Science Laboratory (Yerevan Physics Institute) Foundation, Yerevan, Armenia*
[2]*AGH University of Krakow, Cracow, Poland*
[3]*Bogolyubov Institute for Theoretical Physics, National Academy of Sciences of Ukraine, Kiev, Ukraine*
[4a]*Bose Institute, Department of Physics, Kolkata, India*
[4b]*Centre for Astroparticle Physics and Space Science (CAPSS), Kolkata, India*
[5]*California Polytechnic State University, California, USA*
[6]*Central China Normal University, Wuhan, China*
[7]*Centro de Aplicaciones Tecnológicas y Desarrollo Nuclear (CEADEN), Havana, Cuba*
[8]*Centro de Investigación y de Estudios Avanzados (CINVESTAV), Mexico City and Mérida, Mexico*
[9]*Chicago State University, Chicago, Illinois, USA*
[10]*China Institute of Atomic Energy, Beijing, China*
[11]*China University of Geosciences, Wuhan, China*
[12]*Chungbuk National University, Cheongju, Republic of Korea*
[13]*Comenius University Bratislava, Faculty of Mathematics, Physics and Informatics,*
Bratislava, Slovak Republic
[14]*COMSATS University Islamabad, Islamabad, Pakistan*
[15]*Creighton University, Omaha, Nebraska, USA*

[16]*Department of Physics, Aligarh Muslim University, Aligarh, India*

[17]*Department of Physics, Pusan National University, Pusan, Republic of Korea*

[18]*Department of Physics, Sejong University, Seoul, Republic of Korea*

[19]*Department of Physics, University of California, Berkeley, California, USA*

[20]*Department of Physics, University of Oslo, Oslo, Norway*

[21]*Department of Physics and Technology, University of Bergen, Bergen, Norway*

[22]*Dipartimento di Fisica, Università di Pavia, Pavia, Italy*

[23a]*Dipartimento di Fisica dell'Università, Cagliari, Italy*

[23b]*Sezione INFN, Cagliari, Italy*

[24a]*Dipartimento di Fisica dell'Università, Trieste, Italy*

[24b]*Sezione INFN, Trieste, Italy*

[25a]*Dipartimento di Fisica dell'Università, Turin, Italy*

[25b]*Sezione INFN, Turin, Italy*

[26a]*Dipartimento di Fisica e Astronomia dell'Università, Bologna, Italy*

[26b]*Sezione INFN, Bologna, Italy*

[27a]*Dipartimento di Fisica e Astronomia dell'Università, Catania, Italy*

[27b]*Sezione INFN, Catania, Italy*

[28a]*Dipartimento di Fisica e Astronomia dell'Università, Padova, Italy*

[28b]*Sezione INFN, Padova, Italy*

[29a]*Dipartimento di Fisica "E.R. Caianiello" dell"Università, Salerno, Italy*

[29b]*Gruppo Collegato INFN, Salerno, Italy*

[30]*Dipartimento DISAT del Politecnico and Sezione INFN, Turin, Italy*

[31]*Dipartimento di Scienze MIFT, Università di Messina, Messina, Italy*

[32a]*Dipartimento Interateneo di Fisica "M. Merlin", Bari, Italy*

[32b]*Sezione INFN, Bari, Italy*

[33]*European Organization for Nuclear Research (CERN), Geneva, Switzerland*

[34]*Faculty of Electrical Engineering, Mechanical Engineering and Naval Architecture,
University of Split, Split, Croatia*

[35]*Faculty of Engineering and Science, Western Norway University of Applied Sciences, Bergen, Norway*

[36]*Faculty of Nuclear Sciences and Physical Engineering, Czech Technical University in Prague,
Prague, Czech Republic*

[37]*Faculty of Physics, Sofia University, Sofia, Bulgaria*

[38]*Faculty of Science, P.J. Šafárik University, Košice, Slovak Republic*

[39]*Frankfurt Institute for Advanced Studies, Johann Wolfgang Goethe-Universität Frankfurt,
Frankfurt, Germany*

[40]*Fudan University, Shanghai, China*

[41]*Gangneung-Wonju National University, Gangneung, Republic of Korea*

[42]*Gauhati University, Department of Physics, Guwahati, India*

[43]*Helmholtz-Institut für Strahlen- und Kernphysik, Rheinische Friedrich-Wilhelms-Universität Bonn,
Bonn, Germany*

[44]*Helsinki Institute of Physics (HIP), Helsinki, Finland*

[45]*High Energy Physics Group, Universidad Autónoma de Puebla, Puebla, Mexico*

[46]*Horia Hulubei National Institute of Physics and Nuclear Engineering, Bucharest, Romania*

[47]*HUN-REN Wigner Research Centre for Physics, Budapest, Hungary*

[48]*Indian Institute of Technology Bombay (IIT), Mumbai, India*

[49]*Indian Institute of Technology Indore, Indore, India*

[50]*INFN, Laboratori Nazionali di Frascati, Frascati, Italy*

[51]*INFN, Sezione di Bari, Bari, Italy*

[52]*INFN, Sezione di Bologna, Bologna, Italy*

[53]*INFN, Sezione di Cagliari, Cagliari, Italy*

[54]*INFN, Sezione di Catania, Catania, Italy*

[55]*INFN, Sezione di Padova, Padova, Italy*

[56]*INFN, Sezione di Pavia, Pavia, Italy*

[57]*INFN, Sezione di Torino, Turin, Italy*

[58]*INFN, Sezione di Trieste, Trieste, Italy*

[59]*Inha University, Incheon, Republic of Korea*

[60]*Institute for Gravitational and Subatomic Physics (GRASP), Utrecht University/Nikhef,
Utrecht, Netherlands*

[61]*Institute of Experimental Physics, Slovak Academy of Sciences, Košice, Slovak Republic*

[62]*Institute of Physics, Homi Bhabha National Institute, Bhubaneswar, India*

[63]Institute of Physics of the Czech Academy of Sciences, Prague, Czech Republic

[64]Institute of Space Science (ISS), Bucharest, Romania

[65]Institut für Kernphysik, Johann Wolfgang Goethe-Universität Frankfurt, Frankfurt, Germany

[66]Instituto de Ciencias Nucleares, Universidad Nacional Autónoma de México, Mexico City, Mexico

[67]Instituto de Física, Universidade Federal do Rio Grande do Sul (UFRGS), Porto Alegre, Brazil

[68]Instituto de Física, Universidad Nacional Autónoma de México, Mexico City, Mexico

[69]iThemba LABS, National Research Foundation, Somerset West, South Africa

[70]Jeonbuk National University, Jeonju, Republic of Korea

[71]Johann-Wolfgang-Goethe Universität Frankfurt Institut für Informatik, Fachbereich Informatik und Mathematik, Frankfurt, Germany

[72]Korea Institute of Science and Technology Information, Daejeon, Republic of Korea

[73]KTO Karatay University, Konya, Turkey

[74]Laboratoire de Physique Subatomique et de Cosmologie, Université Grenoble-Alpes, CNRS-IN2P3, Grenoble, France

[75]Lawrence Berkeley National Laboratory, Berkeley, California, USA

[76]Lund University Department of Physics, Division of Particle Physics, Lund, Sweden

[77]Nagasaki Institute of Applied Science, Nagasaki, Japan

[78]Nara Women's University (NWU), Nara, Japan

[79]National and Kapodistrian University of Athens, School of Science, Department of Physics, Athens, Greece

[80]National Centre for Nuclear Research, Warsaw, Poland

[81]National Institute of Science Education and Research, Homi Bhabha National Institute, Jatni, India

[82]National Nuclear Research Center, Baku, Azerbaijan

[83]National Research and Innovation Agency—BRIN, Jakarta, Indonesia

[84]Niels Bohr Institute, University of Copenhagen, Copenhagen, Denmark

[85]Nikhef, National institute for subatomic physics, Amsterdam, Netherlands

[86]Nuclear Physics Group, STFC Daresbury Laboratory, Daresbury, United Kingdom

[87]Nuclear Physics Institute of the Czech Academy of Sciences, Husinec-Řež, Czech Republic

[88]Oak Ridge National Laboratory, Oak Ridge, Tennessee, USA

[89]Ohio State University, Columbus, Ohio, USA

[90]Physics department, Faculty of science, University of Zagreb, Zagreb, Croatia

[91]Physics Department, Panjab University, Chandigarh, India

[92]Physics Department, University of Jammu, Jammu, India

[93]Physics Program and International Institute for Sustainability with Knotted Chiral Meta Matter (SKCM2), Hiroshima University, Hiroshima, Japan

[94]Physikalisches Institut, Eberhard-Karls-Universität Tübingen, Tübingen, Germany

[95]Physikalisches Institut, Ruprecht-Karls-Universität Heidelberg, Heidelberg, Germany

[96]Physik Department, Technische Universität München, Munich, Germany

[97]Politecnico di Bari and Sezione INFN, Bari, Italy

[98]Research Division and ExtreMe Matter Institute EMMI, GSI Helmholtzzentrum für Schwerionenforschung GmbH, Darmstadt, Germany

[99]Saga University, Saga, Japan

[100]Saha Institute of Nuclear Physics, Homi Bhabha National Institute, Kolkata, India

[101]School of Physics and Astronomy, University of Birmingham, Birmingham, United Kingdom

[102]Sección Física, Departamento de Ciencias, Pontificia Universidad Católica del Perú, Lima, Peru

[103]Stefan Meyer Institut für Subatomare Physik (SMI), Vienna, Austria

[104]SUBATECH, IMT Atlantique, Nantes Université, CNRS-IN2P3, Nantes, France

[105]Sungkyunkwan University, Suwon City, Republic of Korea

[106]Suranaree University of Technology, Nakhon Ratchasima, Thailand

[107]Technical University of Košice, Košice, Slovak Republic

[108]The Henryk Niewodniczanski Institute of Nuclear Physics, Polish Academy of Sciences, Cracow, Poland

[109]The University of Texas at Austin, Austin, Texas, USA

[110]Universidad Autónoma de Sinaloa, Culiacán, Mexico

[111]Universidade de São Paulo (USP), São Paulo, Brazil

[112]Universidade Estadual de Campinas (UNICAMP), Campinas, Brazil

[113]Universidade Federal do ABC, Santo Andre, Brazil

[114]Universitatea Nationala de Stiinta si Tehnologie Politehnica Bucuresti, Bucharest, Romania

[115]University of Cape Town, Cape Town, South Africa

[116]University of Derby, Derby, United Kingdom

[117]University of Houston, Houston, Texas, USA

[118]*University of Jyväskylä, Jyväskylä, Finland*
[119]*University of Kansas, Lawrence, Kansas, USA*
[120]*University of Liverpool, Liverpool, United Kingdom*
[121]*University of Science and Technology of China, Hefei, China*
[122]*University of South-Eastern Norway, Kongsberg, Norway*
[123]*University of Tennessee, Knoxville, Tennessee, USA*
[124]*University of the Witwatersrand, Johannesburg, South Africa*
[125]*University of Tokyo, Tokyo, Japan*
[126]*University of Tsukuba, Tsukuba, Japan*
[127]*Universität Münster, Institut für Kernphysik, Münster, Germany*
[128]*Université Clermont Auvergne, CNRS/IN2P3, LPC, Clermont-Ferrand, France*
[129]*Université de Lyon, CNRS/IN2P3, Institut de Physique des 2 Infinis de Lyon, Lyon, France*
[130]*Université de Strasbourg, CNRS, IPHC UMR 7178, F-67000 Strasbourg, France, Strasbourg, France*
[131]*Université Paris-Saclay, Centre d'Etudes de Saclay (CEA),*
IRFU, Départment de Physique Nucléaire (DPhN), Saclay, France
[132]*Université Paris-Saclay, CNRS/IN2P3, IJCLab, Orsay, France*
[133]*Università degli Studi di Foggia, Foggia, Italy*
[134]*Università del Piemonte Orientale, Vercelli, Italy*
[135]*Università di Brescia, Brescia, Italy*
[136]*Variable Energy Cyclotron Centre, Homi Bhabha National Institute, Kolkata, India*
[137]*Warsaw University of Technology, Warsaw, Poland*
[138]*Wayne State University, Detroit, Michigan, USA*
[139]*Yale University, New Haven, Connecticut, USA*
[140]*Yonsei University, Seoul, Republic of Korea*
[141]*Zentrum für Technologie und Transfer (ZTT), Worms, Germany*
[142]*Affiliated with an institute covered by a cooperation agreement with CERN*
[143]*Affiliated with an international laboratory covered by a cooperation agreement with CERN*

[†]Deceased.
[‡]Also at Max-Planck-Institut fur Physik, Munich, Germany.
[§]Also at Italian National Agency for New Technologies, Energy and Sustainable Economic Development (ENEA), Bologna, Italy.
[‖]Also at Dipartimento DET del Politecnico di Torino, Turin, Italy.
[¶]Also at An institution covered by a cooperation agreement with CERN.
[**]Also at Department of Applied Physics, Aligarh Muslim University, Aligarh, India.
[††]Also at Institute of Theoretical Physics, University of Wroclaw, Poland.